Radio Science Bulletin

ISSN 1024-4530

INTERNATIONAL
UNION OF
RADIO SCIENCE

UNION
RADIO-SCIENTIFIQUE
INTERNATIONALE

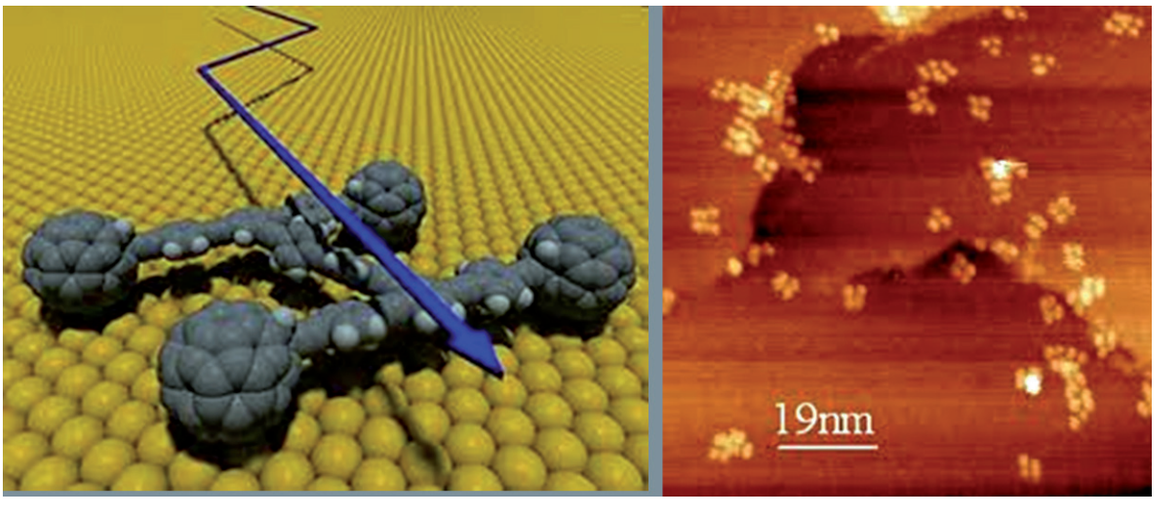

No 341
June 2012

URSI, c/o Ghent University (INTEC)
St.-Pietersnieuwstraat 41, B-9000 Gent (Belgium)

Contents

Front cover: A thermally activated nanocar: (l) the molecular model; (r) the AFM image of an actual ensemble of nanocars. See the paper by Ovidio M. Bucci and Enrico Bucci on pp. 10-21.

For information, please contact :
The URSI Secretariat
c/o Ghent University (INTEC)
Sint-Pietersnieuwstraat 41, B-9000 Gent, Belgium
Tel.: (32) 9-264 33 20, Fax: (32) 9-264 42 88
E-mail: info@ursi.org
http://www.ursi.org

Editorial

Our Papers

At the XXXth URSI General Assembly and Scientific Symposium in Istanbul, Turkey, in 2011, the General Lecture by Per Enge received rave reviews. He has been kind enough to share the material in that lecture with us in this issue of the *Radio Science Bulletin* as an invited paper. The topic is satellite navigation services, including the US Global Positioning System (GPS), and the developing systems from other countries that taken together will constitute a Global Navigation Satellite System (GNSS). The paper begins with a brief review of such systems and their applications. This is followed by a discussion of how frequency diversity is improving both the accuracy and the availability of such systems. The importance and value of the three civilian frequencies associated with such systems is explained, along with the similarities and differences among the various navigation systems in this regard. The impact of such navigation systems on civil aviation is described. The importance of augmentation systems for detecting and correcting faults related to the use of such navigation systems is explained. Ground-, space-, and air-based augmentation systems are covered. The problems created for satellite navigation systems by radio-frequency interference are identified, along with examples of measures taken to mitigate such problems. Finally, an assessment is given for the future of satellite navigation systems. I think you will find this paper as interesting and enjoyable to read as did those who heard the original lecture.

Great advances have been made in recent years in nanotechnology. In their invited *Review of Radio Science* paper from Commission B, Ovidio and Enrico Bucci provide a look at the current and future state of the use of nanotechnology combined with electromagnetic fields for biological diagnosis and treatment. The authors begin with a review of the several ways that electromagnetics are used for diagnosis and treatment in biological systems. They then introduce how nanotechnology – and, in particular, nanoparticles – are changing existing approaches, and opening up possibilities for new approaches. They review microwave imaging. They explain how the use of nanoparticles can enable significantly enhanced contrast in such imaging. Applications to several different types of imaging are described, along with the use of modulation of the probing electromagnetic field that exploits a property of the nanoparticles to significantly improve the sensitivity and resolution of such imaging. The authors then explore the use of nanoparticles with external electromagnetic fields to deliver hyperthermia for the treatment of cancer. The optimization of both the nanoparticles' ability to deliver heat, and of the parameters of the magnetic field used to excite them, are described. This leads to a discussion of the progress and challenges in this interesting new field. The possibility of using bacteria that produce naturally magnetic nanoparticles in such treatments and for other related purposes is explored. The authors present the status and likely future development of the abilities to build, power, and control nanomachines. These could operate at the cellular level in biological systems, with a variety of possible beneficial uses. Nano-hybrids are introduced and explained. These are obtained by coupling a magnetic nanoparticle to a macromolecular structure. Examples of such nano-hybrids that have been successfully produced are given. The paper ends with an examination of the challenges that have to be addressed in this area, and some possible means for addressing them.

The help of Giuliano Manara in providing this invited paper from Commission B is gratefully acknowledged.

Our Other Contributions

Kristian Schlegel has brought us reviews of two books for radio scientists. These reviews were written by two of the Young Scientists from the Istanbul GASS. Their perspectives are particularly welcome.

Zhangwei Wang and James Lin have given us a most interesting contribution to the Radio-Frequency Radiation Safety and Health column. The topic is the calculation of the Specific Absorption Rate (SAR) for portions of the body in MRI systems. This contribution has some important results related to the values obtained in the calculations and their comparisons with limits suggested by regulatory organizations.

We also have calls for papers for several meetings in this issue. In addition, there is the announcement of a special issue of the *Radio Science Bulletin* on the "Role of Radio Science in Disaster Management." I urge you to take advantage of the opportunities offered by these announcements.

In Memoriam

Gert Brussaard
1942 - 2012

Gert Brussaard, Professor Emeritus at the Technical University of Eindhoven and Past President of URSI, died of cancer on May 22, 2012.

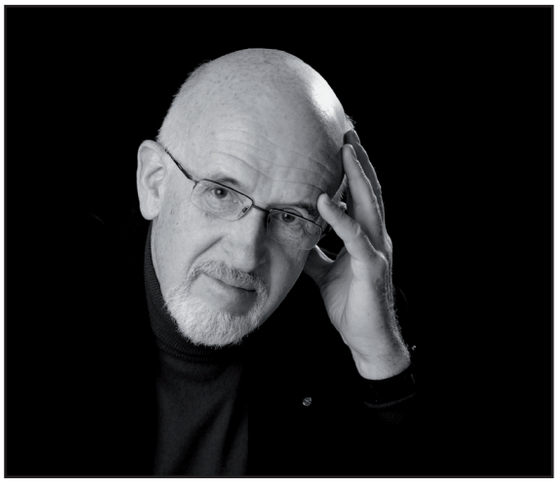

Gert Brussaard was born in Zegveld, the Netherlands, on October 5, 1942. He received the Master of Science Degree in Electrical Engineering from Delft University of Technology in 1966. From 1966 to 1968, he did his military service with the Royal Netherlands Air Force, working on Technical Intelligence. From 1968 to 1974, he worked with the Dr. Neher Laboratory of the Netherlands PTT. There, he was responsible for experimental radio propagation research in support of the design of HF systems, microwave radio links, and satellite communication systems. Together with the Satellite Communications group, he was responsible for the design and construction of the experimental Earth station of PTT Research used in the SIRIO and OTS satellite projects. In 1969, he became involved in the work of CCIR Study Group 5 on propagation. Later, when CCIR became ITU-R, he was appointed Chair of Working Party 3J, responsible for radio-propagation fundamentals.

From July 1974 until October 1988, he was with ESTEC, the technical center of the European Space Agency (ESA). He was instrumental in creating the Electromagnetics Division inside the Electrical Engineering Department of ESA. As Head of the Wave Interaction and Propagation Section, he was responsible for the implementation of a European research program in wave propagation modeling in support of satellite-communication and remote-sensing systems.

In 1985, he obtained his PhD degree in Applied Sciences from the Université Catholique de Louvain in Louvain la Neuve, Belgium. His thesis was entitled "Radiometry – A Useful Prediction Tool?" This concluded a 10-year research project on microwave radiometry.

In October 1988, he joined the Technical University of Eindhoven, the Netherlands, as a full professor in Radiocommunications. He became Head of the Telecommunications Division at the Faculty of Electrical Engineering. After his retirement from the University in July 2002, he worked as a consultant, and he kept giving lectures at the Royal Military Academy of the Netherlands.

In 2004, he was appointed Chair of the Technical Committee for Telecommunications, Information Science and Technology of the European research program COST. He was well known and respected in COST circles, having been Vice Chair of two COST Actions (25/4 and 205), and having served as the Dutch delegate in a number of other COST actions.

From 1990 to 1993, he was Chair of URSI Commission F. As Associate Scientific Program Coordinator of the 2002 URSI General Assembly in Maastricht, he took responsibility for the quality of this important event, and successfully enlisted several of the main sponsors of the event. For the 2005 URSI General Assembly in New Delhi, he was again responsible for the scientific program.

At the 2008 URSI General Assembly in Chicago, he was elected President of URSI: he was the first Dutchman in this position. Due to ill health, he was not able to serve the full term of three years.

He was a Senior Member of the IEEE, a member of the Royal Institute of Engineers of the Netherlands, and a member of the Netherlands Radio Engineering and Electronics Society. He was also a member of the Health Council of the Netherlands and its Commission for Electromagnetic Fields.

Besides his professional activities, Gert was an active member of the Rotary Club Heeze and of the Vederfonds foundation. He had numerous other interests, from singing in choirs to flying single-engine airplanes. He was an avid sportsman, running the New York Marathon and the famous "elf-steden tocht:" the ice-skating marathon that passes 11 cities in Friesland. He was also an enthusiastic skier. When an ITU meeting in Geneva happened to be in winter, he always used the opportunity to visit the mountains. I had the privilege not only to work with him, but also to ski with him and his family, and to enjoy his camaraderie and good humor. He is survived by his wife, Virginia, and his sons Anne, Seth, and Martin.

Bertram Arbesser-Rastburg
E-mail: bertram.arbesser-rastburg@esa.int

Satellite Navigation : Present and Future

Per Enge

Abstract

The Global Positioning System serves one billion civil users, with applications including navigation for cars, aircraft, ships, spacecraft, pedestrians, and emergency services; time transfer for telecommunications, finance, and power delivery; and a breadth of scientific uses. Cognizant of this utility, the Russians are rejuvenating their satellite navigation system, and new systems are being fielded by China, Japan, India, and Europe. Taken together, this Global Navigation Satellite System will provide geometric diversity, with over one hundred navigation satellites, all with triple frequency diversity for civil use. This paper will briefly describe the technology, with a focus on aviation applications.

1. Introduction

Satellite navigation serves a wide breadth of applications, based on the satellites depicted in Figure 1. As shown, the vast majority of these satellites are in medium Earth orbit (MEO), with some assistance from satellites in geostationary orbits (GEO). In 2011, most of these satellites belonged to the Global Positioning System (GPS), originally developed by the US Department of Defense. This development began in the 1970s, when the planners predicted that GPS would serve a total of 40,000 military users, with some ancillary civil use. Today, the civil community ships over ten million GPS receivers per month. The GPS tail now wags the dog, and the civil community has generated an unexpected breadth of applications.

For example, every new Boeing or Airbus aircraft carries a GPS receiver for navigation in the enroute and terminal-area airspaces. GPS is also used to guide aircraft while approaching airports. In some cases, it provides the most critical vertical dimension of location down to altitudes of 200 feet.

In addition, most new smart phones or feature phones carry GPS receivers that have a bill of materials around $1.00. These receivers are used to guide our walking and driving lives. They also automatically provide our location to emergency services when we make such a call. In time, they will provide our location to good Samaritans standing next to automatic electronic defibrillators when someone suffers a heart attack. GPS receivers in cell phones will also serve significantly less uplifting applications that push advertising to our phones, based on our location.

Other applications include ship navigation, pointing information for spacecraft, land survey, energy exploration; and time transfer for telecommunications, power delivery, and financial transactions.

Attracted by this utility, Russia is rejuvenating their satellite navigation system, called GLONASS. China is expanding their regional system, Beidou (also known as Compass), to include global coverage. Europe has launched their first prototype satellites for the Galileo system. Japan and India have launched satellites for the regional systems. Figure 2 depicts a satellite-navigation future based on over one hundred satellites from this family of systems. Taken together, we will have a Global Navigation Satellite System (GNSS).

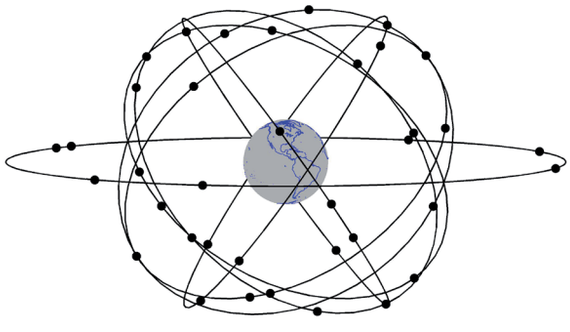

Figure 1. Today, GPS has approximately 32 satellites in medium Earth orbit. GPS is augmented by seven satellites in geostationary orbit (from [1, 2]).

Per Enge is with Stanford University, Stanford, CA, USA; e-mail: penge@stanford.edu. *This paper was one of the invited General Lectures presented at the URSI General Assembly and Scientific Symposium, August 2011, Istanbul, Turkey*

[Note: An earlier version of this paper was included in the record of a GNSS workshop sponsored by the US National Academy of Engineering and the Chinese Academy of Engineering in May of 2011. The title was "Global Navigational Satellite Systems."]

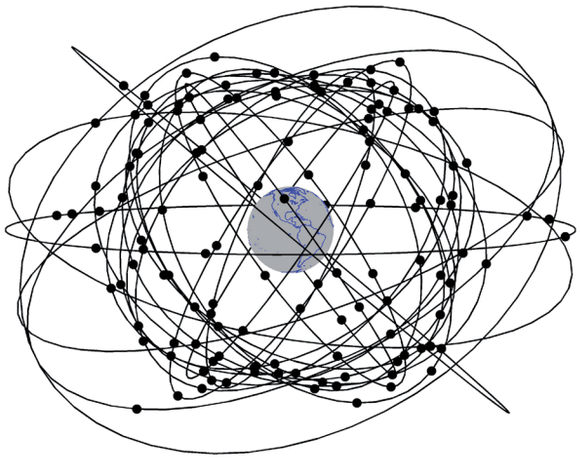

Figure 2. In the next generation, GNSS may grow to include over 100 satellites, mostly in medium Earth orbit, with some in geostationary and inclined elliptical orbits (from [1, 2]).

Section 2 of this paper describes the new signals to be delivered by this multiplicity of constellations. Section 3 focuses on my area of greatest interest: civil aviation. Section 4 discusses our continuing concern with radio-frequency interference (RFI), and Section 5 is a brief summary.

2. Frequency Diversity for Satellite Navigation

The multiplicity of satellites described above will provide geometric diversity. Happily, the new satellites will also provide frequency diversity for civil users. Each new satellite will radiate civil signals at three frequencies, rather than the single civil frequency offered today.

The top trace in Figure 3 shows the spectrum for the GPS satellites that are currently being launched. These new satellites broadcast at three civil frequencies: L1, L2, and L5. L1 is 1575.42 MHz, and home for the so-called clear-access (C/A) signal. This signal has a spread spectrum with a modest chipping rate of 1 Mcps. Even so, it is the basis for all of the civil applications described above. L1 C/A overlays military signals in this same band. L2 is 1227.60 MHz, and also carries a civil signal with a 1 Mcps chipping rate on the seven most recent GPS satellites. Taken together, L1 and L2 provide redundancy to combat accidental radio-frequency interference (RFI), and a means to remove the dispersive delay due to the ionosphere. Both features are important. Radio-frequency interference is becoming more prevalent in the GPS bands, and the ionosphere is the largest natural error source.

At 1176.45 MHz, L5 is the home for the first civil signal with a 10 Mcps chipping rate. It provides 10 dB more processing gain against radio-frequency interference, and can be used with L1 to remove the ionospheric delay. L1 and L5 are particularly important to aviation. They both fall in Aeronautical Radio Navigation System (ARNS) portions of the radio spectrum. Unlike L2, these ARNS signals may be used by civil aircraft to provide navigation in poor visibility as part of instrument flight rules (IFR). Taken as a triplet, L1/L2/L5 allow receivers to form beat-frequency signals that can be used to resolve the carrier phase ambiguity and enable phase interferometric measurements for very high precision.

The signals for GLONASS, Galileo, and Compass are also shown in Figure 3. As shown, they are not identical to the GPS signal shown in the top trace. However, they share the main features: triple frequency diversity, with at least two signals in ARNS bands surrounding L1 and L5.

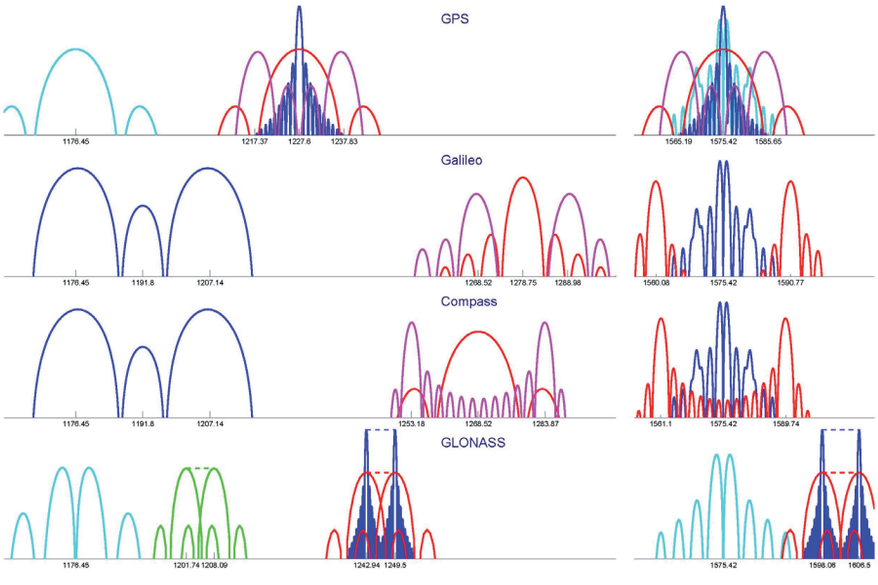

Figure 3. The signal spectra for GPS, Galileo, Compass, and GLONASS. From the left, new GPS satellites radiate at L5 (1176.45 MHz), L2 (1227.60 MHz,) and L1 (1575.42 MHz) (from [1]).

3. Impact on Civil Aviation

Civil aviation has augmented GPS to detect faults or rare normal conditions that threaten flight safety. Faults are failures in the manmade portions of our navigation systems. The probability of a fault in the GPS system is approximately $10^{-5}/\text{hour}$ per satellite. The target level of safety for an aircraft navigation system is approximately 10^{-7} per hour, or one hundred times smaller than the observed failure rate. Similarly, rare normal conditions, notably the ionosphere, can introduce location errors that may be potentially hazardous to aircraft safety. These can occur several times per year during the peak of the solar cycle. In these peak years, the rate of these events is more than one hundred times greater than the target level of safety for aviation. Hence, the civil-aviation community has augmented GPS with systems that detect and remove errors due to these faults and rare normal conditions. Three such augmentation strategies exist.

Ground-based augmentation systems (GBAS) are located at the airport to be served. Reference receivers monitor the GPS (or GNSS) signals. Since the reference receivers are at known locations, they can generate corrections to remove the nominal GPS errors, and they can generate alarms to flag satellites that cannot be reasonably corrected and characterized. All the reference receivers are on the airport property. The corrections and alarms are thus only valid within 100 km or so around the airport. We call this the terminal airspace. Given this limitation on range of applicability, ground-based augmentation systems use a VHF data broadcast to communicate with nearby aircraft.

Space-based augmentation systems (SBAS) spread their reference receivers across continental areas. For example, some 38 stations are used to cover North America. These receivers send their GPS measurement data to master stations, which generate corrections and error-bounding data that are valid over the area spanned by the reference network. Since the data are valid over continental areas, space-based augmentation systems use a geostationary satellite to broadcast this navigation safety data to the airborne fleet.

In contrast to space-based augmentation systems and ground-based augmentation systems, aircraft-based augmentation systems (ABAS) are self contained. In fact, aircraft-based augmentation systems include a family of fault-detection techniques known as receiver autonomous integrity monitoring (RAIM). Space-based augmentation systems and ground-based augmentation systems detect faults by comparing the GPS measurements to ground truth. Receiver autonomous integrity monitoring compares the GPS measurement from one satellite to the consensus of the other satellites in view. Mathematically, receiver autonomous integrity monitoring is based on the residuals of the individual GPS measurements relative to the least-squares navigation solution based on all satellites in view. Receiver autonomous integrity monitoring is attractive because it does not need a ground reference network or a real-time broadcast from the ground network to the aircraft. However, the receiver autonomous integrity monitoring fault-detection capability is weak compared to space-based augmentation systems or ground-based augmentation systems, because it does not have access to ground truth. The navigation solution must be over-specified, and the geometries of the underlying subset solutions must be strong. Receiver autonomous integrity monitoring has thus not yet been used for vertical guidance. It has only been approved for lateral guidance.

With the advent of the new constellations described above, receiver autonomous integrity monitoring may be able to support vertical navigation. After all, geometric diversity means that the navigation solutions will be over-specified and that the subset geometries will be stronger. The air navigation community is researching this possibility, and has developed a concept imaginatively known as advanced receiver autonomous integrity monitoring, or ARAIM. Importantly, this set of algorithms includes a set of requirements on the core GNSS constellations. These requirements must be met and verified daily if the core constellation is to be included in the suite of measurements used by the avionics to support vertical navigation.

If advanced receiver autonomous integrity monitoring can be proven to be safe, then it may be able to support navigation down to altitudes of only one hundred feet over the airport's surface. Since advanced receiver autonomous integrity monitoring would be a multi-constellation capability, it would be independent of the health of any one of the core GNSS constellations. Today, air navigation based on GPS requires 22 or more GPS satellites, but the Department of Defense only guarantees 21 satellites.

4. Radio-Frequency Interference

As mentioned earlier, GPS satellites broadcast from medium Earth orbit (MEO), and so the satellites are approximately 12,000 miles above the receivers. These satellites are placed at this altitude so that an individual satellite covers one-third of the Earth's surface. With 30 satellites carefully arranged in medium Earth orbit, all earthbound users of GPS (with a clear view of the sky) can see at least the prerequisite four satellites to instantaneously determine three dimensions of location plus time. Medium Earth orbit is used so that a reasonably sized constellation can enable navigation worldwide.

However, medium-Earth-orbit signals are weak when they reach the Earth, and GNSS signals have a received power of only 10^{-16} W. They can be easily overwhelmed by Earth-sourced interfering transmissions at the GPS frequency. This radio-frequency interference (RFI) can be *scheduled*, *accidental*, or *malevolent*. Amongst these,

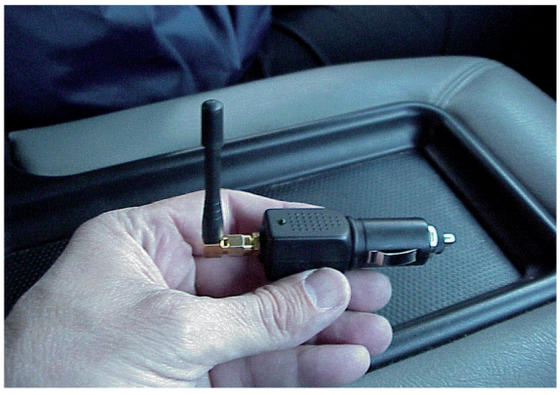

Figure 4. An example of a personal privacy device (PPD).

deliberate interference, called jamming, is the looming threat.

In the past year, so-called personal privacy devices (PPDs) have become widely available on the Internet, and such a jammer is shown in Figure 4. The most inexpensive personal privacy devices are single-antenna devices that jam the one GPS signal frequency (L1) that is used by most users. More-expensive units have multiple antennas, and attack all three GPS signal frequencies (L1, L2, and L5). As such, these attackers anticipate the next generation of GPS user equipment that would continue to function if only one or two of the three frequencies were jammed. Other personal privacy devices jam GPS and the cell-phone frequencies at the same time, shutting down all calls. They are preferred by car thieves that wish to prevent on-car warning systems from reporting the GPS location of a stolen car to the authorities.

Personal privacy devices range in price from $30 to over $300, based on the number of frequencies under attack and the transmitted power. They radiate powers from a few milliwatts to hundreds of milliwatts. The former knock out GPS receivers for hundreds of yards, and the latter can have dangerous effects for many miles.

As their name suggests, personal privacy devices are marketed to individuals that fear for their privacy. This sales strategy seems to be effective. An investigation recently initiated by the Federal Aviation Administration (FAA) revealed that trucks traveling on the New Jersey Turnpike carry these devices. The drivers perhaps worry that the company dispatcher is monitoring their locations. Ironically, the attention of the dispatcher must be drawn to the truck that never provides location reports.

In any event, a personal privacy device can cause collateral damage much greater than any privacy protection the user may possibly enjoy. The above-mentioned FAA investigation was sparked while a ground-based augmentation system was being installed at Newark International Airport. As described above, ground-based augmentation systems use GPS receivers at the airport to aid GPS receivers in the approaching aircraft. The ground-based augmentation system's antennas were placed next to the New Jersey Turnpike, and the ground receivers suffered frequent continuity breaks during the test period. These breaks were due to personal privacy devices carried by vehicles on the New Jersey Turnpike. The United States is currently investigating legal and technical remedies for personal privacy devices. At Newark, the antennas will be relocated, and the system will be reconfigured to better tolerate short outages on a subset of the antennas.

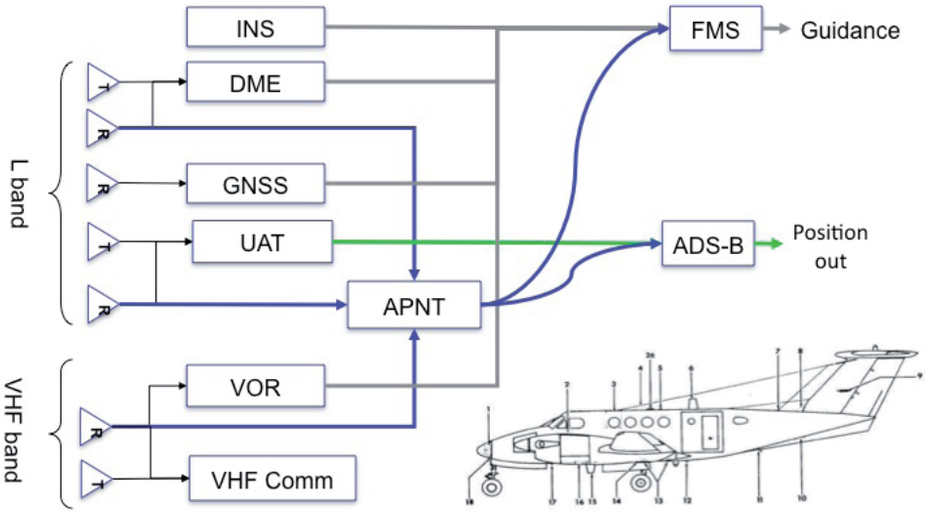

Figure 5. Potential sources of alternate position, navigation, and time (APNT), including inertial navigation systems (INS), distance-measuring equipment (DME), a universal-access transponder (UAT), VHF omnidirectional radio (VOR), and VHF communications.

For the longer term, the FAA focuses on alternate position navigation and time (APNT) based on terrestrial radio navigation and inertial navigation. Today, the aviation community continues to operate the full set of terrestrial navigation aids that predated GPS. These include VHF omnidirectional range (VOR), distance-measuring equipment (DME) and instrument landing systems (ILS). If GPS is jammed or suffers from some other systemic failure, pilots can revert to these systems. However, this terrestrial network is expensive, and it does not support the navigation capabilities needed for the Next-Generation Air Traffic Management System (NextGen). It needs to be reconfigured to reduce cost and provide area navigation rather than point-to-point navigation. NextGen is predicated on area navigation, which is not fully backed up by today's ground-based network.

To this end, the alternate position navigation and time effort focuses on the provision of area navigation for all enroute and terminal airspace over CONUS, and approach navigation for all airports required for safety and commerce. Alternate position navigation and time should be independent of GNSS. Rather, it should be based on navigation aids that can be cost-effectively retained or are planned for installation in the next decade. This investigation has included all of the navigation aids shown in Figure 5, and has focused on distance-measuring equipment (DME) and ground-based transmitters planned for the next generation of surveillance.

5. Summary

GPS serves well, with approximately one billion users utilizing a surprising breadth of applications. In the future, the capability of satellite navigation will multiply as GPS is joined by a rejuvenated system from Russia, and new systems from China, Europe, Japan, and India. This multiplicity of ranging sources will provide geometric diversity. Moreover, each of these satellites will radiate ranging signals for civilians at three or more frequencies, and some of these new signals will have ten times the bandwidth of the GPS C/A code signal that enables the vast majority of present applications. We can thus expect a new wave of applications that leverage these new technical capabilities. However, radio-frequency interference will be a continuing challenge. Concern for privacy is great, and so jammers designed to protect privacy will wreak collateral havoc.

6. References

1. Liang Heng, *Safe Satellite Navigation with Multiple Constellations: Global Monitoring of GPS and GLONASS Signal-In-Space Faults*, Stanford PhD dissertation, 2012.

2. Frank Van Diggelen, *A-GPS: Assisted GPS, GNSS and SBAS*, Norwood, MA, Artech House, 2009.

Electromagnetism, Nanotechnologies and Biology : New Challenges and Opportunities

Ovidio M. Bucci
Enrico Bucci

Abstract

This paper reviews the possibilities offered by the advent of nanotechnology for regulating the interaction between electromagnetic fields and bio-systems with unprecedented flexibility and specificity. In particular, we discuss how the exploitation of magnetic nanoparticles and magnetic fields can lead to significant advances in clinical and diagnostic applications, and to the opening of a completely new scenario: the true remote control of nanomachines and biological systems.

1. Introduction

Bioelectromagnetics – i.e., the study of interactions between non-optical electromagnetic fields (EMF) and biological systems – has attracted considerable interest since the discovery of electrical and magnetic phenomena. The goal is to exploit these interactions in medical diagnostics and therapy, or for detecting possible health hazards. Following the evolution of biological knowledge, the research proceeded in a top-down way, from organisms, to tissues, cells, and single biological macromolecules. The main results of the huge effort dedicated to investigate the existence of possible adverse effects of non-ionizing radiation were summarized in the well known ICNIRP reports [1, 2], while examples of clinical applications are magnetotherapy [3] and hyperthermia [4].

As for clinical diagnostics, magnetic-resonance imaging (MRI) stands as the most successful exploitation of electromagnetic-field interaction with biological systems. More recently, microwave imaging (MWI) has been proposed as a complementary diagnostic imaging tool, mainly for cancer detection [5].

Besides the somehow serendipitous attempt to identify biological effects beneficial to health – with the notable exception of MRI – the efforts to develop diagnostic and therapeutic electromagnetic-field applications have been focused on the realization of effective exposure devices and protocols, without any attempt to modify the electromagnetic properties of the target system in order to improve the performance of the desired applications. As examples of this kind of approach, consider the nuclear magnetic-resonance techniques developed to study the response of atomic nuclei to the magnetic field. The intent was to infer the three-dimensional structure of biological macromolecules – the above-mentioned microwave imaging – to get a conductivity and permittivity map of a target's tissue for breast-cancer detection, the mapping of the electrical activity of different organs (hearth, brain, skin) to examine their functionality.

The advent of nanotechnologies, with the possibility of producing nanometer-size particles able to efficiently interact with the electromagnetic field, while being biocompatible and linkable to a large number of macromolecular systems with different properties, opens up a new scenario. As a matter of fact, the nanometric size of these components allows specific targeting of electromagnetic-field-active nanoparticles to the region of interest (ROI) in a selected biosystem [6] without obstacles from physical barriers. This introduces the possibility of controlling and regulating the electromagnetic field's interaction with nanometric-size biocomponents, i.e., with the majority of biomolecular machinery. This possibility can not only significantly improve the performance of existing techniques – as already happened for MRI – but may lead to the development of completely new techniques, for both clinical and biotechnological applications.

Ovidio M. Bucci is with the Dipartimento di Ingegneria Biomedica, Elettronica e Telecomunicazioni, University of Naples Federico II, via Claudio 21, 80125 Napoli, Italy; and the Istituto di Ricerca sul Rilevamento Elettromagnetico dell'Ambiente (IREA-CNR), via Diocleziano 328, 80127 Napoli, Italy; e-mail: bucci@unina.it. Enrico Bucci is with the Istituto di Biostrutture e Bioimmagini – CNR, Via Mezzocannone, 16 – 80131, Napoli, Italy; e-mail: enrico.bucci@unina.it.

This paper is one of the invited Commission B Reviews of Radio Science.

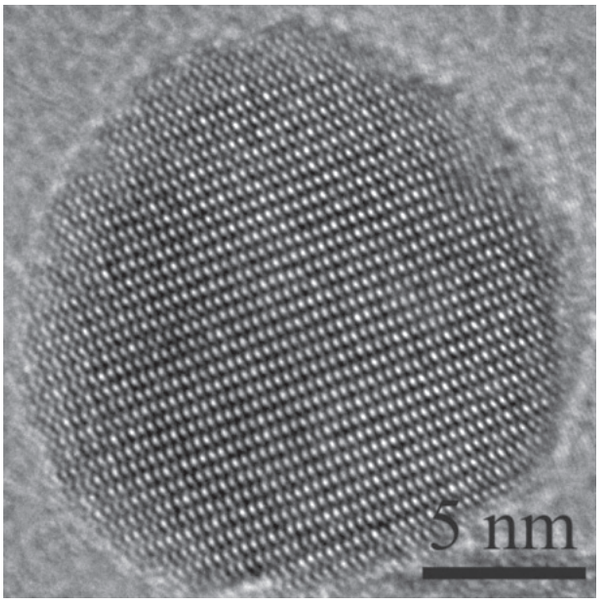

Figure 1. A transmission electron microscopy image of an Fe_3O_4 magnetic nanoparticle.

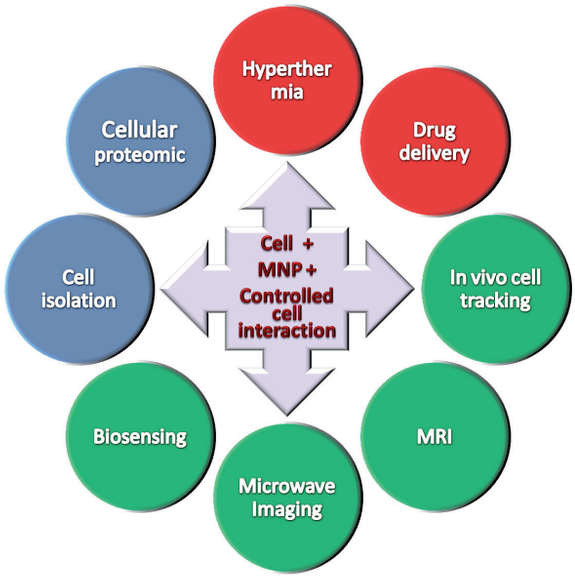

Figure 2. Magnetic nanoparticle applications that exist or are under development.

The currently available electromagnetic-field-active nanoparticles that have been shown to be linkable to macromolecular systems include carbon nanotubes [7] and a range of magnetic nanoparticles (MNPs), some of them approved by FDA for use in humans. Magnetic nanoparticles have the further advantage of strongly interacting with magnetic fields over a wide band, from microwaves down to very low frequencies, thus allowing minimization of unwanted interactions with biological systems.

Magnetic nanoparticles are very stable, pseudo-spherical crystallites of magnetic material (typically, ferromagnetic material). They are usually covered with polymers, ranging in size from few nm to some μm (see Figure 1). Magnetic nanoparticles are ideally suited to mediate the interaction between an applied magnetic field and the biological system because:

a. They are compatible with most of the chemistry used for attaching well-described targeting molecules;

b. They allow the selective modification of the electromagnetic properties of a specific region of interest in an otherwise transparent background, simplifying both the visualization of the region of interest and the confinement of the electromagnetic-field effects to this region;

c. They can thermally dissipate the energy acquired by an external field, providing a way to trigger a desired response by a temperature-sensitive biological target;

d. They can exert mechanical actions when subject to a proper external electromagnetic field.

Due to the above appealing features, a number of possible applications have been developed or proposed, as depicted in Figure 2.

In the following, we will examine how the above characteristics can be exploited to improve the performance of some existing techniques, or to develop completely new techniques. In particular, in Section 2, we will consider the use of magnetic nanoparticles as a contrast agent for improving microwave-imaging applications. In Section 3, we will briefly illustrate the possibilities in the field of magnetic-nanoparticle hyperthermia, both in the medical and biotechnological fields. In Section 4, we will discuss the possibility of using magnetic nanoparticles as key components of remotely controlled and powered nanomachines for biotechnological applications.

2. Microwave Imaging

Microwave imaging exploits the dependence of the electromagnetic field scattered by an object on its electromagnetic parameters (i.e., the relative permittivity and conductivity). Microwave imaging aims at obtaining a map of the values of the electromagnetic parameters from scattered-field data, collected under a suitable set of primary illuminations. Due to the relationships existing among the dielectric features of the tissue and its physio-pathological status [8], microwave imaging has a diagnostic potential for assessing tissue conditions associated with such dielectric changes [9]. Given the aforementioned characteristics, microwave imaging has been particularly oriented to the diagnosis of nodular formations in breast cancer, which is difficult at low resolution and limited depth. As compared to X-ray and MRI techniques, microwave imaging does not use ionizing radiation, involves relatively cheap and portable apparatus, and offers minor patient discomfort.

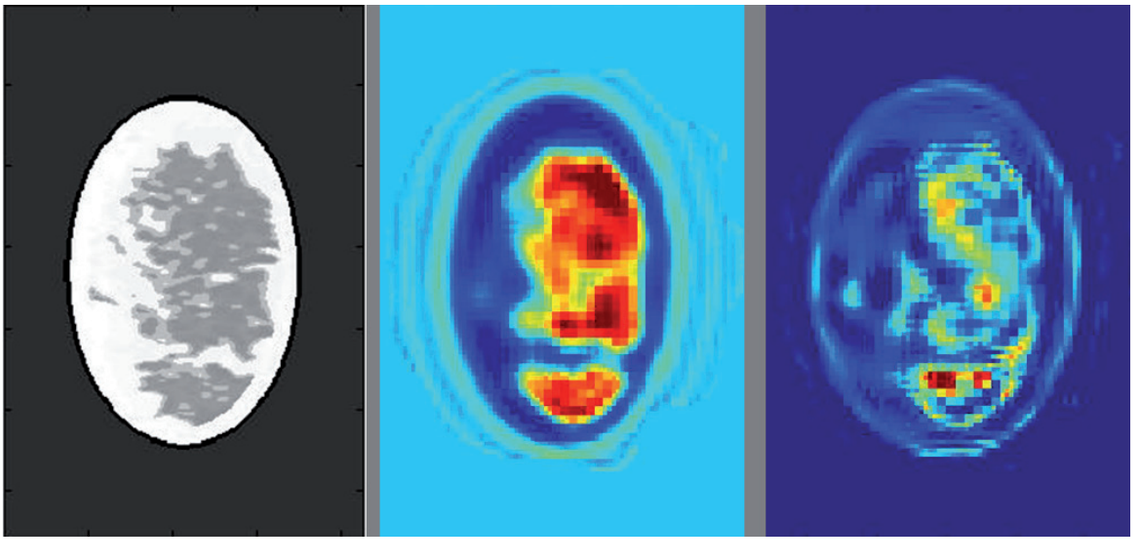

Figure 3. Images of a very dense female breast: (l) MRI; (c) microwave imaging (permittivity); (r) microwave imaging (conductivity) (from I. Catapano, R. Scapaticci, and L. Crocco, "Wavelet-Based Adaptive Multiresolution Inversion for Quantitative Microwave Imaging of Breast Tissues," submitted to IEEE Transactions on Antennas and Propagation; courtesy of the authors).

Accordingly, a strong effort has been dedicated in the last years to develop effective imaging algorithms, able to deal with the mathematical and computational difficulties of the *nonlinear* inverse-scattering problem involved. An example of the achievable results is shown in Figure 3, wherein the microwave image is compared with a corresponding MRI image.

However, recent studies of the dielectric properties of human mammary tissues at microwave frequencies [10] have outlined that while there is a remarkable contrast among cancerous and healthy fatty tissues, such a difference drastically decreases when malignant and normal glandular/fibro-connective tissues are compared. As a consequence, microwave imaging may fail in discriminating between these two kinds of tissues.

Similar to other medical imaging techniques, the adoption of selective agents to increase the electric contrast between cancerous and healthy tissues has been proposed to overcome this difficulty [11-14]. However, the actual possibility of selectively achieving significant contrast increases is by no means obvious. The biocompatibility of the proposed agents is an open question, so that none of these is yet allowed for clinical use. To overcome these difficulties, a new contrast-enhanced microwave-imaging methodology, exploiting magnetic nanoparticles as a contrast agent, was very recently proposed [15]. Due to the nonmagnetic nature of human tissues, the capability of producing a magnetic anomaly localized only in the tumor represents a powerful and specific way to avoid ambiguities in discriminating between cancerous and healthy tissues.

The use of magnetic nanoparticles as a magnetic contrast agent was already proposed and exploited in magnetic-particle imaging (MPI) [16], an imaging technology that is currently under active industrial development in the pre-clinical field. Magnetic-particle imaging uses a time-constant, spatially inhomogeneous magnetic field (the driving field), and a radiofrequency, spatially uniform field (the modulation field). The driving field is large enough to saturate the magnetic nanoparticles except in a narrow spatial region, called the null-field zone (NFZ), wherein it vanishes. The modulation field has an amplitude large enough to induce a nonlinear response of the magnetic nanoparticles. Hence, no field is scattered by the magnetic nanoparticles outside the null-field zone, while a field containing higher-order harmonics is scattered by magnetic nanoparticles falling in the null-field zone. The imaging is then performed by moving the null-field zone over the investigated zone, and detecting the scattered signal for each spatial position.

While achieving a resolution of few millimeters in detecting the magnetic anomaly, magnetic-particle imaging is unable to image the surrounding tissues. This is because it operates at kHz frequencies. It has thus been integrated with MRI, thus inheriting the drawbacks of this last technique in terms of cost and portability. Moreover, due to constraints posed by the breast geometry, the possibility of obtaining a well-localized null-field zone over all the region of interest with an external, localized apparatus is by no means obvious [17].

These drawbacks are not present in magnetic-nanoparticle contrast-enhanced microwave imaging. However, due to the limited amount of magnetic nanoparticles that can be homed into tumors, only marginal contrast increases can be expected by selective targeting. Since the induced anomaly is embedded into a strong surrounding electrical scenario (SES), the amplitude of the signal that is meaningful for diagnostics purposes (i.e., the scattered field arising from the targeted tumor) may be several orders of magnitude lower than the actually measured

signal, which instead accounts for *both* the surrounding electrical scenario and the tumor. As a consequence, the possibility of recovering the magnetic contribution cannot rely on a straightforward comparison between the field scattered before and after the addition of the magnetic nanoparticles. This is because even small errors in the geometrical and/or electromagnetic characterization of the measurement setup, or minor variations in the surrounding electrical scenario (due, for instance, to patient movements), would completely hinder the contribution sought.

To face this problem, a feature of magnetic nanoparticles peculiar to their behavior in the microwave frequency range – that is, the dependence of their magnetic susceptibility on an external polarizing magnetic field (PMF) [18] – can be exploited [19]. Due to this property, the electromagnetic response of magnetic nanoparticles – and henceforth their contribution to the overall signal – can be driven by means of a polarizing magnetic field. In particular, modulating the polarizing magnetic field induces a corresponding modulation of the contribution associated with the magnetic contrast, which allows its extraction from the measured signal.

In practice, the simplest modulation can be obtained by switching off the magnetic response by applying an external polarizing magnetic field of sufficient intensity. Since *on-off* switching and data collecting can be performed very quickly, no significant variation can occur either in the measurement setup or in the surrounding electrical scenario, so that the difference between the *on* and *off* data actually provides the contribution due to the magnetic nanoparticles. This is the crucial feature of the envisaged procedure, as it allows the extraction of the useful signal in the presence of a much stronger co-occurring signal, provided the precision of the measurement apparatus is sufficient and the noise is lower than the useful signal. A scheme using this *on-off* strategy is reported in Figure 4.

In Figure 4, χ_e and χ_m respectively denote the electric and magnetic contrasts relative to the surrounding electrical scenario end-targeted tumor. It must be stressed that because the induced magnetic anomaly can be safely treated as a weak scatterer, its imaging can be faced by exploiting a *linear* inversion strategy, once the electrical characteristics of the surrounding electrical scenario (either estimated or provided by a standard microwave-imaging algorithm) are known. This implies a great reduction in complexity and computational burden as compared with standard microwave imaging. However, as the inversion requires the knowledge of the permittivity and conductivity of the region of interest, the algorithm must be sufficiently insensitive to the unavoidable errors in the estimation of the electric scenario.

Preliminary numerical results obtained following this approach were promising [19, 20]. They showed the possibility of imaging realistic magnetic-nanoparticle concentrations, even if only a very rough knowledge of the surrounding electrical scenario was available. An example is shown in Figure 5 (adapted from [20]). This referred to the case of a tumor with a diameter of 1 cm (shown in black), with a concentration of magnetic nanoparticles of 10 mg/cm^3, located in different positions inside a simplified breast phantom. The reconstruction of the magnetic contrast was carried out assuming that *no information* on the

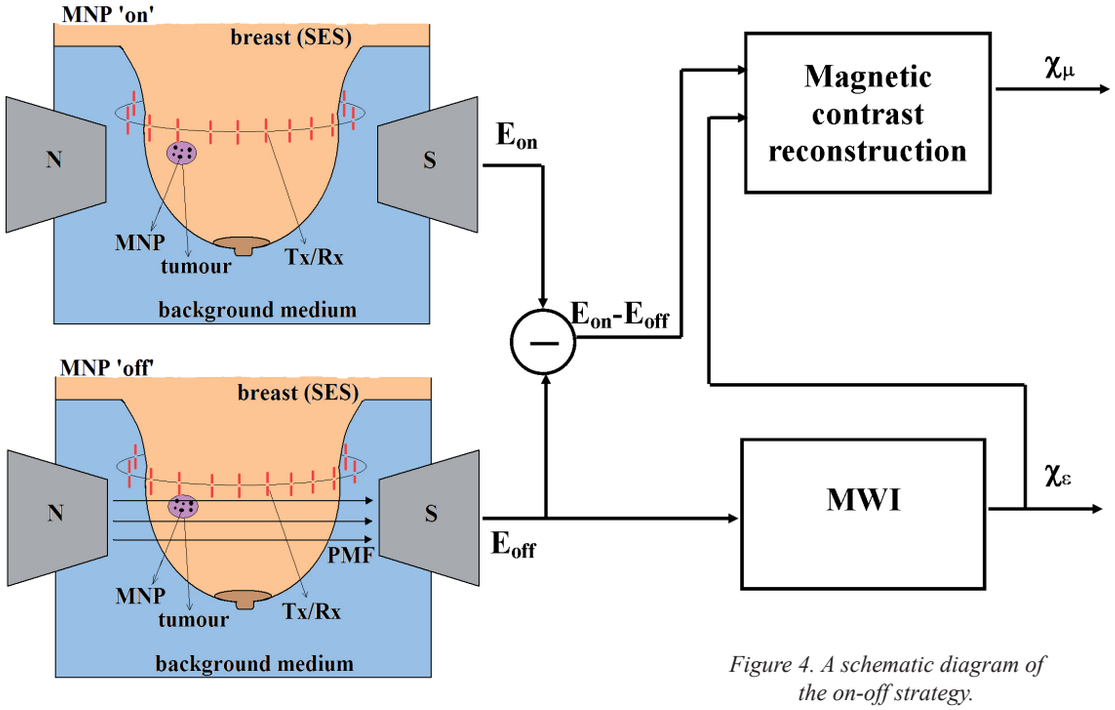

Figure 4. A schematic diagram of the on-off strategy.

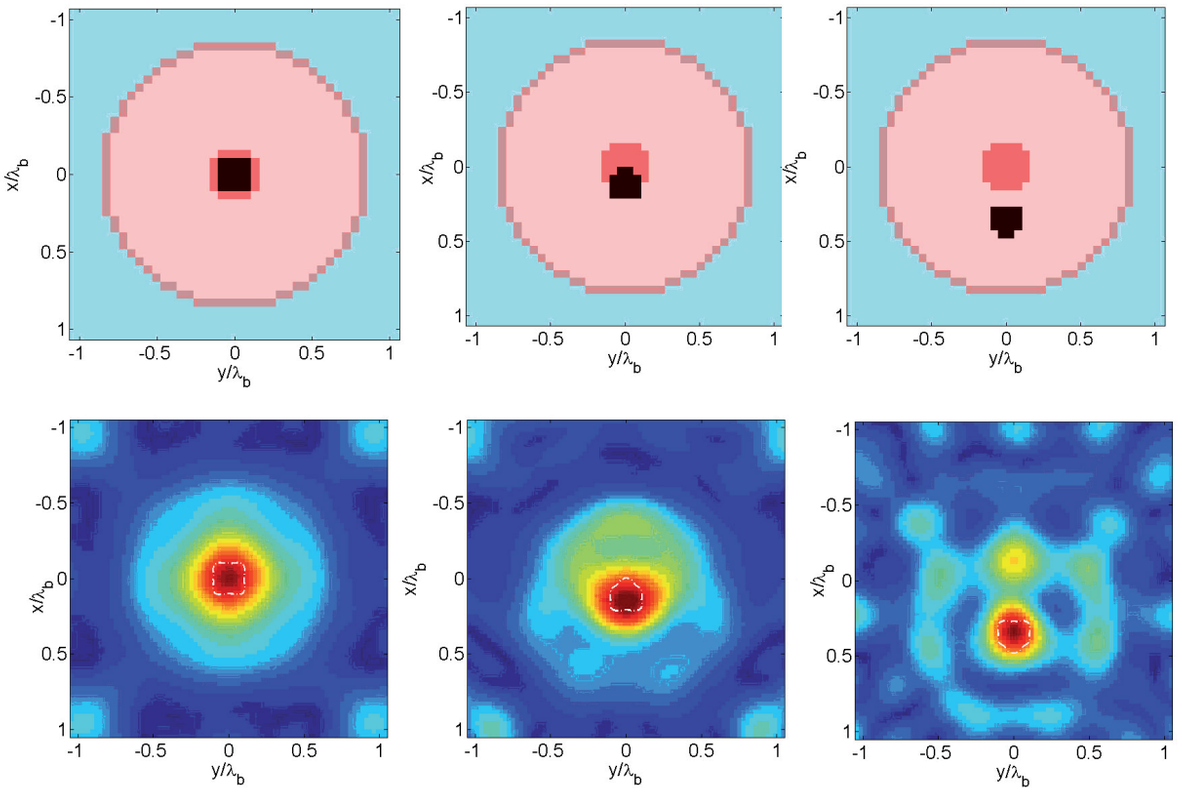

Figure 5. Imaging of a tumor targeted with magnetic nanoparticles inside a simplified breast phantom, using the on-off strategy,

surrounding electrical scenario was available, hence adopting for its electric properties those of the surrounding matching fluid. Not withstanding this extreme assumption, by comparing the original phantoms (upper row) and the corresponding images of the magnetic anomaly (lower row), we could see that the tumor was correctly detected and located.

Due to the low level of the field scattered by the magnetic nanoparticles, high dynamical ranges and signal-to-noise ratios are required by the measurement apparatus. These could be possibly reduced by exploiting both more-complex polarizing magnetic-field modulations and the knowledge of the magnetic nanoparticles' spectral response, which should allow devising a "matched-filter" approach for recovering the magnetic contribution. Moreover, it is anticipated that the availability of magnetic nanoparticles with different spectral responses could allow the development of a "multi-color" imaging modality, with different magnetic nanoparticles targeting different pathology markers in the region of interest.

3. Magnetic-Field Hyperthermia

Even more than their bulky magnetic counterparts, magnetic nanoparticles can thermally dissipate the energy acquired from an applied oscillating electromagnetic field. At a sufficiently high concentration, this can in turn cause a local increase in temperature, i.e., a hyperthermal effect.

Biological systems at all dimensional scales are sensitive to the external temperature, providing the basis for a controlled induction of a certain range of effects by magnetic hyperthermia. One of these effects consists of the induction of cellular death, or the sensitization of the cell to other insults, such as chemical agents. Another effect consists of the activation of a series of transcriptional programs, which usually brings the production of protective proteins by the cell under thermal shock. By targeting the magnetic nanoparticles to cancerous cells, the first effect can be used to improve oncological therapies. By genetically engineering a cell so as to change the proteins that will be produced under thermal shock, one can get a remotely-switchable bioreactor to produce a desired product, without changing the bulk temperature of the medium.

Let us examine the first of these two possibilities, i.e., clinical hyperthermia [4]. This kind of therapeutic intervention relies on the well-established fact that it is possible to induce damage or necrosis of cancerous cells by elevating their temperature above 42°-48°C and keeping it elevated for approximately thirty minutes [21]. Hyperthermia also increases the sensitivity of the cancerous cells to some therapeutic agents, such as ionizing radiation and certain cytotoxic drugs [21]. Hyperthermia's combined use with radiotherapy and/or chemotherapy can thus significantly improve the efficacy of these anticancer treatments.

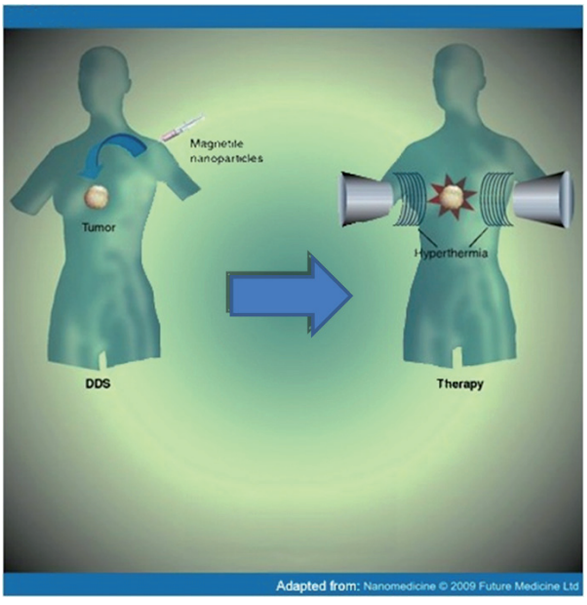

Figure 6. A basic sketch of magnetic-nanoparticle hyperthermia.

Among the modalities of anticancer hyperthermia proposed until now is magnetic-nanoparticle hyperthermia (MNPH) [21]. This technique (see Figure 6), which exploits the heat generated by magnetic nanoparticles when subjected to an applied radio-frequency (RF) magnetic field (MF), appears to be one of the most promising techniques, due to:

1. The high capability of the magnetic nanoparticles to convert the energy of an applied field into heat [22];

2. The possibility of selectively concentrating the magnetic nanoparticles at the cancer site by minimally invasive routes [23];

3. The high transparency of the human tissues to RF magnetic fields.

Indeed, thanks to these features, magnetic-nanoparticle hyperthermia could allow achieving highly selective and homogeneous heating of the cancerous tissue, above the therapeutic temperature, even for tumors deeply sited in the body, something otherwise unachievable by means of other approaches. In addition, compared to systemic and regional hyperthermia, magnetic-nanoparticle hyperthermia has several advantages. This is because local heating can achieve higher temperatures, causes only limited patient discomfort [24], and does not induce fever-like effects on the immune system [25].

Despite promising results in animal models, few clinical trials on humans have been performed. These have been done mainly on an empirical basis. Only limited successes in treating cancer of the prostate [24], brain [26], and different recurrent tumors [27] have been achieved.

To firmly establish a more rational basis before entering new clinical studies, two major and strictly related aspects need to be addressed [28]. The first concerns the optimization of both the magnetic nanoparticles' heat-generating properties (depending on the composition of the magnetic nanoparticles, and their diameter, d), and the magnetic-field parameters (the intensity, H, and the frequency, f). The second aspect is the estimation of the limits of clinical scalability of the treatment, namely the minimum tumor size and the maximum extension of the region of the body exposed to the applied field (irradiated tissues) that can be safely and effectively treated.

For a given composition of magnetic nanoparticles, the estimation of the optimal values for H, f, and d is not an easy task. This is because it is required that the heating produced by the induced electric currents over the irradiated tissues be limited in order to preserve the integrity of the healthy tissue exposed to the applied field. It is these constraints, together with the limit in the maximal achievable concentration of magnetic nanoparticles at the tumor site, which set the limits of the clinical scalability.

As a matter of fact, the amount of magnetic nanoparticles required for selective heating increases both when tumors of decreasing size are treated (in order to balance the higher capability of smaller tumors to dissipate heating towards the neighboring tissues), and when the extension of the irradiated tissue grows (in order to compensate for the larger amount of non-selective heating produced, via the Joule effect, by the electric field). There thus exists a minimum tumor size and a maximum exposure-region size – related to the maximum achievable concentration of magnetic nanoparticles – beyond which cancer cannot be safely and successfully treated. These points have recently been theoretically addressed, presenting a criterion for the optimal choice of the values of H, f, and d [29]. These are the values requiring the minimal amount of magnetic nanoparticles into the tumor, taking into account both the heat-generating properties of the magnetic nanoparticles and the heat-transfer processes. By applying this criterion to a simplified yet realistic model, some significant results have been obtained. In particular, it was found that for magnetite magnetic nanoparticles:

1. Values of Hf larger than the safety threshold of 4.85×10^{8} $\mathrm{Am^{-1}s^{-1}}$ usually considered in the literature can be adopted.

2. The optimal diameters for the magnetic nanoparticles lie in the range of 16-20 nm, in agreement with the experimental data reported in [30].

3. For concentrations of available magnetic nanoparticles that typically can be reached today (≈10 mg/ml), magnetic-nanoparticle hyperthermia is unable to treat malignancies with a radius smaller than about 3.5 mm. To reach this limit, the radius of the exposed region cannot exceed about 5 cm.

4. For a tumor radius larger than 7 mm, no practical limit exists for the extension of the irradiated region, and thus the treatment does not require previous knowledge of the tumor localization.

5. Concentrations even smaller than about 3 mg/ml can be used, as long as sufficiently monodisperse magnetic nanoparticles, moderately perfused tissues, and/or suitable magnetic-field amplitudes are involved.

These results point to the main challenges that must be faced to obtain a reliable clinical relevance for magnetic-nanoparticle hyperthermia, i.e.,:

1. The design of an exposure device able to focus the magnetic field as much as possible, while shaping it in such a way as to minimize the corresponding induced electric field.

2. An increase of about one order of magnitude in the achievable concentration of magnetic nanoparticles, so as to target cancer of about 1.5 mm in radius, which is a relevant clinical goal.

3. Alternatively, improving by one order of magnitude the heat-generating properties of magnetic nanoparticles by varying their chemical composition [30].

Let us now turn to the description of some possible biotechnological applications of magnetic-nanoparticle hyperthermia.

As anticipated, it has long been known that cells can respond to an external increase in temperature by activating specific genes and producing the corresponding proteins. Since the ability of a gene to respond to temperature is coded into a defined DNA sequence, a genetic engineer can build synthetic DNA sequences having these temperature-responsive elements attached to whatever gene is of interest. The obtained synthetic DNA is in turn introduced into a proper bacterial cell, which will synthesize the corresponding protein only when the external temperature is set above a certain threshold. While this approach is straightforward at a relatively small scale, homogeneously and quickly heating the solution containing the bacterial cells in industrial volumes – which range in scale from hundreds to thousands of liters – is quite problematic and costly. This drawback could be overcome if one could produce a selective local heating of the bacterial colonies (which can grow up to many centimeters in size with a very high cellular density) without heating the bulk solution.

There are now bacteria strains that can produce natural magnetic nanoparticles that are very homogeneous and with suitable magnetic properties [31], while some of the bacteria strains currently used for biotech production can be functionalized with a very high number of magnetic nanoparticles [32]. For this reason, the use of these magnetic bacteria has been proposed for biotechnological applications. A further advantage of using such an approach would be the easy recovery of the bacterial cells containing the target protein, simplifying the elimination of the solution media and thus the first purification steps.

While this approach has been proposed on the basis of the magnetic characterization of both the naturally magnetic bacteria and the bacteria functionalized with magnetic nanoparticles [33], a full theoretical evaluation of the hyperthermal effects, similar to what has been produced for clinical applications, is needed before entering into practical experimentation.

4. Toward New Applications: Powering and Controlling Nanomachines

Cellular activity – and thus life – is the final result of the coordinated work of an unimaginably high number of tiny molecular devices, which range in size from few to hundreds of nanometers. In the case of man, there are about 30,000 different types of such nanometric devices (the proteins). These are often found in complexes with other macromolecules to form biological nanomachines, i.e., devices of nanometric size operating at a nanometer scale. The cells are able to perform their tasks by controlling both the mechanical movements of specific internal components of such nanomachines (to switch them on and off), and their overall translation at target sites (to concentrate their activity where required). Therefore, being able to *build*, *power*, and *control* nanomachines would disclose an incredible number of diverse applications, well behind the exploitation of cellular factories typical of current molecular-biology applications.

As for *building* nanomachines, there has been significant work in investigating the possibility of designing complex molecular architectures, starting from a range of available synthetic components such as carbon-cage structures, DNA, and organometallic compounds. This flood of miniaturized designs constituted a source of inspiration for the chemists, which indeed developed a series of synthetic strategies leading to the realization of a variety of nanometric architectures. Remarkably, many of these were inspired by macroscopic counterparts, such as molecular motors, cantilevers, valves, shuttles, scissors, barrows, elevators, and recently, nanovehicles [34-37].

As for *powering* nanomachines, it must be recalled here that biological machines are mostly powered by electrochemical potentials, and, in a few cases, by optical radiation. Therefore, first attempts have been focused on imitating the cell: powering nanomachines by means of pH or ionic-strength changes, molecular fuels, light, or even thermal agitation (Brownian motors). Two examples are shown in Figures 7 and 8. Figure 7 (adapted from [34]) refers to an optically activated molecular rotor. A molecular complex is chemically linked to a gold surface from one

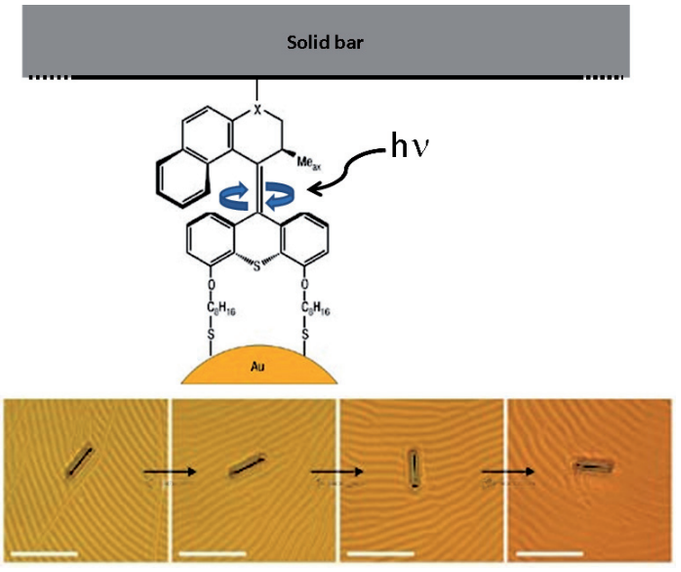

Figure 7. An optically activated molecular rotor.

side, and to a solid (much bigger) bar on the other side. In the middle of the rotor, there is a chemical bond, which is the axis of the rotor. When the rotor is irradiated by UV, it enters in an excited, high-energy electronic state. This relaxes back to a stable ground state by a 180° clockwise rotation around the axis, as shown in the (optical) microscopy images at the bottom. of Figure 7. Figure 8 (adapted from [35]) shows a nanocar activated by thermal agitation. The nanocar wheels, made of Buckminsterfullerene (C60), can rotate without sliding on a gold surface.

However, all of the above-mentioned fuelling approaches suffer from one or more drawbacks, namely:

1. The adverse effects of chemical fuelling, which limits the applications involving living organisms.

2. The irreversible poisoning of the solution, which limits the number of cycles of activity available for the nanomachine.

3. The necessity to provide the fuel, preventing all those applications where the fuel is not available directly in the solution and cannot be easily added to it.

4. In the case of optical powering, the limited penetration and the damaging effects of the required high-energy UV radiation.

5. In the case of Brownian motors, the very nature of the powering, which does not allow any control of the work cycle.

As for *controlling* nanomachines, it is clear that a type of control with high penetration that does not modify the environment and can be remotely activated is obviously preferred. To this aim, different mechanisms have been proposed and tested, exploiting electrical-field gradients [36]. This approach is nevertheless limited to applications where the solvent used is non-polar and does not contain ions, so that no ionic currents are induced in the solution.

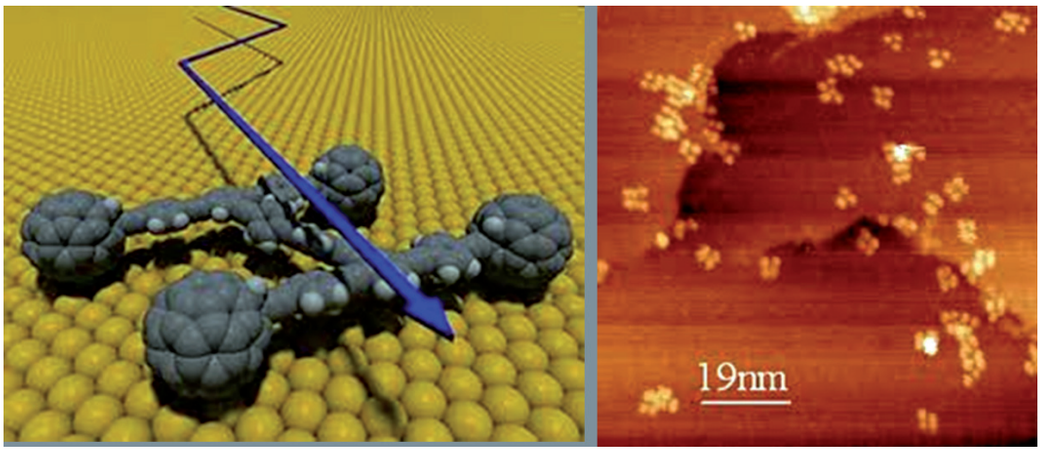

Figure 8. A thermally activated nanocar: (l) the molecular model; (r) the AFM image of an actual ensemble of nanocars.

Moreover, when biological systems are involved, several if not all of the solution components are charged, and thus are prone to unwanted electrophoretic effects induced by the applied electrical gradients.

To overcome the aforementioned powering and controlling difficulties, a possible solution could be the use of an external magnetic field. In this way, it would be possible to maintain all the advantages of a remote powering and control system, without the above-mentioned limitations. This would also have the extra advantage of a very selective control of the nanomachines for medical applications, since living tissues are transparent to magnetic fields at sufficiently low frequencies.

As pointed out in the Introduction, the use of magnetic nanoparticles as transducers appears to be the best solution. This is due to their small size, comparable to nanomachines; their versatile chemistry, which allows linking them to the nanomachines; and the high capability of interaction, either energetically or mechanically, with an applied magnetic field. Concerning the last point, at least in principle, both of the interaction mechanisms could be exploited to realize magnetically driven nanomachines. However, it has been shown that the mechanisms of energy transfer from the magnetic nanoparticles to an attached macromolecule are generally so inefficient [38, 39] and the relaxation times by which the macromolecule transfers the energy to the solvent are so short [40] as to prevent the possibility of using this type of interaction. Accordingly, at present, the only practical way to realize magnetically controlled nanomachines appears to be a direct mechanical action through the magnetic nanoparticles [41]. This is done by transferring linear or angular mechanical momentum to the whole nanomachine (i.e., without involving internal degrees of freedom), so to induce stretching, rotation, and/or movement of it or a part of it.

To stretch a suitable biological macromolecule – such as a DNA duplex – up to producing a useful conformational change – such as the opening of the double helix – requires forces of the order of some tens of pN [42]. Forces much stronger must be applied to modify the geometry of more-compact biological objects, such as the proteins. The maximum force that can be exerted on magnetic nanoparticles is equal to $M_s V_m \left|\mathrm{grad}\, B\right|$, with M_s being the saturation magnetization of the nanoparticle ($M_s \approx 480$ kAm^{-1} for a magnetite nanoparticle), and V_m being its volume.

Accordingly, extremely high field gradients are required to exert the above forces using magnetic nanoparticles of a size lower than 100 nm, as needed for macromolecule-size nanomachines. These gradients can only be obtained in regions of interest of micrometric size. For larger nanomachines, such as multi-molecular biological systems (e.g., magnetically modified viruses), this limit can obviously be relaxed. This is because larger magnetic cores can be used, as are currently made for micrometer-size magnetic tweezers [43].

Beside using it to control the motion of some nanomachine part, a force can be used to translate the nanomachine from one point to another. The force needed in this case is much smaller, since the only resistance to the motion are the Brownian forces deriving from thermal agitation, which are orders-of-magnitude smaller [42]. Moreover, a proper magnetic-field gradient can be used to confine a magnetic nanoparticle to a given position with nanometric precision [45, 46].

Such control of the magnetic nanoparticle's position can be used in a way that is analogous to the transport and localization of biologically active macromolecules to defined sites actuated by the cell. This can be deployed in a similar way as a means to control a fully structured nanofactory, where magnetic-nanoparticle-functionalized nanomachines are transported to an "active" site, exert their work (or are modified by the local environment), and are subsequently translated to a different position. The relevant difference is that the entire process can be operated *remotely*, as opposite to cells, which operate *locally* (by means of sequential local alterations of the cytoskeleton for transport and of vesicles for confinement).

While the forces that can be exerted on a magnetic nanoparticle are not useful for causing structural changes in nanomachines smaller than 100 nm, torques can be used to this aim. At this scale, the magnetic nanoparticles consist of a single magnetic domain (SD), and behave as stable permanently magnetic dipoles [47]. In the absence of an external magnetic field, the magnetic moment of a stable single-domain magnetic nanoparticle with *uniaxial anisotropy* is directed along a preferred direction, called the *easy-magnetization axis*, which is fixed with respect to the magnetic nanoparticle. When a magnetic field is applied along a direction not parallel to the easy-magnetization axis – due to the torque exerted by the applied magnetic field – the magnetic dipole of the magnetic nanoparticle, initially directed along the easy-magnetization axis, will deviate from this direction. This deviation will cause a mechanical torque on the magnetic nanoparticle. Accordingly, due to the anisotropy, the application of an external magnetic field results in a mechanical torque acting on the magnetic nanoparticle that can induce a rotation of the magnetic nanoparticle as a whole.

The maximum torque that can be exerted is equal to $K_a V_m$ [41], wherein the constant, K_a, called the anisotropy constant, depends on the chemical constitution of the magnetic nanoparticle ($K_a \approx 15$ kJ/m^3 in the case of magnetite). To exert such a torque, the applied magnetic field must be larger than $2K_a/\mu_0 M_s$. Accordingly, torques up to some nN nm can be obtained with reasonable field intensities (of the order of 10^5 Am^{-1}). For comparison, the torque required to unwind a DNA duplex is about 10 pN nm [48], while that needed to operate the ATP synthase is of the order of 50 pN nm, so that the use of magnetic nanoparticles as magnetically driven rotors in nano-hybrids appears most promising [41].

After this brief overview of the mechanisms available for powering and controlling both the activity and position of a magnetic nanoparticle using a magnetic field, let us examine some of the nano-hybrids that have actually been obtained by coupling a magnetic nanoparticle to some proper macromolecular structure. While most of these are only able to exploit magnetophoretic effects [49] without the activation of internal motors or the controlled movement of part of the machine to achieve a desired effect, they can still be thought of as components of nanomachines different from what had been originally conceived.

The simplest nano-hybrids consist of a magnetic nanoparticle coupled to a biological macromolecule via a different type of covalent bonding strategy, such as carbodiimide activation. It has been proven that the biological component preserves its structure and activity [50, 51], so that the resulting nano-hybrid can be transported to a preferred site of action via magnetophoresis. As previously reported, the nanometric precision recently achieved in translating such nanohybrids and in confining them to a predetermined site render this very simple magnetic nanoparticle-nanomachine already attractive for on-chip applications and building of nanofactories. However, in these examples, the geometry of the resulting nano-hybrids is poorly controlled, because of the fact that the orientation between the magnetic axis and the biomolecule is random – not to mention the difficulty in obtaining by chemical synthesis a mono-functionalized magnetic nanoparticle.

In an attempt to obtain more-defined geometries, biotechnologists have used viruses, which are made of an exact number of proteins arranged in a very defined geometry. Since a virus auto-assembles in a sequential number of repetitive steps from its constituent proteins, if these proteins carry an attached nanoparticle, an ordered structure of magnetic-nanoparticle proteins is obtained (i.e., a magnetic virus), with sizes ranging from about 200 to 500 nm. For rod-shaped viruses, such as the tobacco mosaic virus [52], every magnetic nanoparticle attached to more than a single protein, or attached to a protein in the wrong position, is automatically excluded from the process, bringing to an abortive virus before the completion of the assembling process. Moreover, during the assembling process, the magnetic nanoparticles are disposed in a linear string, a fact that possibly orients their magnetic moments along the virus' axis, building up a bigger resulting magnetic moment. By further modifying the constituent proteins of these viruses, it is conceivable that these magnetic viruses could be incorporated in bigger nanomachines, as magnetic components with a precise geometry and orientation with respect to the other parts of the nanomachine.

Trying to obtain nanocomponents with the same characteristics but at smaller size has been recently attempted by growing magnetite nanocrystals in the interior of the protein ferritin. While the protein mostly preserved its geometry – which was known at atomic detail – the number and orientation of the magnetic domains in its interior could not be controlled. This resulted in a decreased total magnetic moment and a poorly controlled magnetic anisotropy [53]. However, it is worth noting that while the magnetoferritin obtained could not be used as a component of a nanomachine's motor, it still may be used for actuation by magnetic gradients. In this respect, having a very small magnetic component (with a diameter of the range of 10 nm), which exposes a proteic shell, can be very useful for applications in vivo.

However, to successfully design and build an effective magnetically driven nanomachine based on the use of these components, a set of points must be addressed. In particular, as discussed in [41]:

1. The internal (movement of the magnetic moment with respect to the magnetic nanoparticle) and external (overall particle motion) dynamics of the magnetic nanoparticle in the presence of an external, variable, magnetic field, and of the external resistant couple exerted by the nanomachine, must be accurately modeled and dealt with, taking into account thermal fluctuations.

2. The relevant macroscopic degrees of freedom of the nanomachine and their dynamics must be accurately modeled and dealt with, taking into account internal dissipation as well as thermal fluctuations.

3. The proper orientation between the magnetic nanoparticle, the rotation axis of the external magnetic field, and the transmission axis mast be ensured when assembling the nanomachine.

Achieving a successful assembly with respect to point 3 is particularly challenging, due to the presence of Brownian motions of the components to be assembled, and the existence of very strong, short-range surface effects that dominate chemical interactions at such dimensional scales. The magnetic field could possibly also be exploited to alleviate these difficulties, since, as previously discussed, the field can be used to precisely position magnetic nanoparticles from one side, as well as to orient them by exploiting magnetic anisotropy.

On the basis of the aforementioned considerations, it is reasonable to foresee that the actual realization of remotely controlled nanomachines is not too far in the future.

In the light of this perspective, a final remark is in order, concerning the peculiar risks connected with the possibility of being fully successful in achieving the goal of complete and remote control of a molecular biosystem. To illustrate this point, let us consider very recent results obtained in the field, i.e., the remote control of the activity of an ionic channel (the protein TRPV1) by the combined use of magnetic nanoparticles and the electromagnetic field [54]. Briefly, a population of neuronal cells expressing TRPV1 was selectively covered with magnetic nanoparticles, anchored to the cellular membrane (where TRPV1 resides).

Under stimulation by an alternating magnetic field, it has been proven without any doubt that TRPV1 was activated, causing an influx of calcium into the neuron, which was fully measurable after 15 seconds. When the same type of neurons were labeled by magnetic nanoparticles in vivo, i.e., in the brain of the humble roundworm Caenorhabditis elegans, stimulation by an electromagnetic field caused a very rapid retraction and bending of the worm. This behavior is very well known to be caused by that particular type of neuron. Notwithstanding the fact that the mechanism proposed by the authors for the activation of TRPV1 by the excited magnetic nanoparticle was possibly wrong, the data were compelling, excluding experimental artifacts. In this respect, this particular set of experiments represented a seminal work in the field, and a triumph in translating the remote control of biosystems very far. However, the protein used, TRPV1, is an ionic channel mediating pain and burning sensations. This work can therefore be considered the first successful attempt to control an organism with a central nervous system by remotely induced pain to cause a fugue behavior.

5. References

1. International Commission on Non-Ionizing Radiation Protection, "Exposure to High Frequency Electromagnetic Fields, Biological Effects and Health Consequences (100 kHz - 300 GHz) – Review of the Scientific Evidence and Health Consequences," *ICNIRP Reports*, 2009.

2. International Commission on Non-Ionizing Radiation Protection, "Exposure to Static and Low Frequency Electromagnetic Fields, Biological Effects and Health Consequences (0-100 kHz) – Review of the Scientific Evidence and Health Consequences," *ICNIRP Reports*, 2003.

3. R. J. Linovitz, M. Pathria, M. Bernhardt, D. Green, M. D. Law, R. A. McGuire, P. X. Montesano, G. Rechtine, R. M. Salib, J. T. Ryaby, J. S. Faden, R. Ponder, L. R. Muenz, F. P. Magee, and S. A. Garfin, "Combined Magnetic Fields Accelerate and Increase Spine Fusion: A Double-Blind, Randomized, Placebo Controlled Study," *Spine*, **27**, 13, 2002, pp.1383-9.

4. R. A. Vertree, A. Leeth, M. Girouard, J. D. Roach, and J. B. Zwischenberger, "Whole-Body Hyperthermia: A Review of Theory, Design and Application," *Perfusion*, **17**, 4, 2002, pp. 279-90.

5. S. Semenov, "Microwave Tomography: Review of the Progress Towards Clinical Applications," *Philos. Transact. A Math. Phys. Eng. Sci.*, **367**, 1900, 2009, pp. 3021-42.

6. G. Saravanakumar, K. Kim, J. H. Park, K. Rhee, and I. C. Kwon "Current Status of Nanoparticle-Based Imaging Agents for Early Diagnosis of Cancer and Atherosclerosis," *J. Biomed. Nanotechnol*., **5**, 1, 2009, pp. 20-35.

7. A. Mashal, B. Sitharaman, J. H. Booske, and S. C. Hagness, "Dielectric Characterization of Carbon Nanotube Contrast Agents for Microwave Breast Cancer Detection," IEEE International Symposium on Antennas and Propagation, Charleston, SC, USA, June 2009.

8. K. R. Foster and H. P. Schwan, "Dielectric Properties of Tissues and Biological Materials. A Critical Review," *Crit. Rev. Biomed. Eng.,* **17***,* 1, 1989, pp. *25-104*.

9. E. C. Fear, P. M. Meaney and M. A. Stuchly, "Microwaves for Breast Cancer Detection?" *IEEE Potentials*, **22**, 1, 2003, pp. 12-18.

10. M. Lazebnik, D. Popovic, L. McCartney, C. B. Watkins, M. J. Lindstrom, J. Harter, S. Sewall, T. Ogilvie, A. Magliocco, T. M. Breslin, W. Temple, D. Mew, J. H. Booske, M. Okoniewski, and S. C. Hagness, "A Large-Scale Study of the Ultrawideband Microwave Dielectric Properties of Normal, Benign and Malignant Breast Tissues Obtained from Cancer Surgeries," *Phys. Med. Biol.*, **52**, 2007, pp. 6093-6115.

11. S. Semenov, N. Pham, and S. Egot-Lemaire, "Ferroelectric Nanoparticles for Contrast Enhancement Microwave Tomography: Feasibility Assessment for Detection of Lung Cancer," World Congress on Medical Physics and Biomedical Engineering, Munich, Germany, September 2009.

12. A. Mashal et al., "Toward Carbon-Nanotube-Based Theranostic Agents for Microwave Detection and Treatment of Breast Cancer: Enhanced Dielectric and Heating Response of Tissues-Mimicking Materials," *IEEE Transactions on Biomedical Engineering*, **57**, 8, 2010, pp.1831-1834.

13. J. D. Shea, P. Kosmas, B. D. Van Veen, and S. C. Hagness, "Contrast-Enhanced Microwave Imaging of Breast Tumors: A Computational Study Using 3D Realistic Numerical Phantoms," *Inverse Problems*, **26**, 7, 2010, pp. 1-22.

14. M. Klemm, J. Leendertz, D. Gibbins, I. J. Craddock, A. Preece, and R. Benjamin, "Towards Contrast Enhanced Breast Imaging Using Ultra-Wideband Microwave Radar System," Proceedings of the 2010 IEEE Radio and Wireless Symposium (RWS'10), 2010, pp. 516-519.

15. G. Bellizzi, O. Bucci, I. Catapano, "Microwave Cancer Imaging Exploiting Magnetic Nanoparticles as Contrast Agents," *IEEE Transactions on Biomedical Engineering*, **59**, 9, 2011, pp. 2528-2536.

16. B. Gleich and J. Weizenecker, "Tomographic Imaging Using the Nonlinear Response of Magnetic Particles," *Nature*, **435**, 2005, pp. 1214-1217.

17. T. F. Sattel, T. Knopp, S. Biederer, B. Gleich, J. Weizenecker, J. Borgert, and T. M. Buzug, "Single-Sided Device for Magnetic Particle Imaging," *J. Phys. D: Appl. Phys.*, **42**, 3, 2009, p. 022001 (5 pp.).

18. P. C. Fannin, "Use of Ferromagnetic Resonance Measurements in Magnetic Fluids," *J. of Molecular Liquids*, **114**, April 2004, pp.79-87.

19. G. Bellizzi, O. M. Bucci, and I. Catapano, "Magnetic Nanoparticle as Contrast Agent for Microwave Breast Cancer Imaging," Proceedings of the Fourth European Conference on Antennas and Propagation (EuCAP), Barcelona, Spain, 2010, pp.1-5.

20. G. Bellizzi, O. M. Bucci, and I. Catapano, "Microwave Cancer Imaging Exploiting Magnetic Nanoparticles as Contrast Agents," *IEEE Transactions on Biomedical Engineering*, **58**, 9, 2011, pp. 2528-2536.

21. A. Jordan, R. Scholz, K. Maier-Hauff, M. Johannsen, P. Wust, J. Nadobny, H. Schirra, H. Schmidt, S. Deger, S.A. Loening, W. Lanksch, and R. Felix, "Presentation of a New Magnetic Field Therapy System for the Treatment of Human Solid Tumors with Magnetic Fluid Hyperthermia," *Journal of Magnetism and Magnetic Materials*, **225**, 2001, pp.118-126.

22. R. E. Rosensweig, "Heating Magnetic Fluid with Alternating Magnetic Field," *Journal of Magnetism and Magnetic Materials*, **252**, 2002, pp. 370-374.

23. S. J. DeNardo, G. L. DeNardo, A. Natarajan, L. A. Miers, A. R. Foreman, C. Gruettner, G. N. Adamson, and R. Ivkov, "Thermal Dosimetry Predictive of Efficacy of 111In-ChL6 Nanoparticle AMF-Induced Thermoablative Therapy for Human Breast Cancer in Mice," *J. Nucl. Med.*, **48**, 2007, pp. 437-444.

24. M. Johannsen, U. Gneveckow, K. Taymoorian, B. Thiesen, N. Waldöfner, R. Scholz, K. Jung, A. Jordan, P. Wust, and S. A. Loening, "Morbidity and Quality of Life During Thermotherapy Using Magnetic Nanoparticles in Locally Recurrent Prostate Cancer: Results of a Prospective Phase I Trial," *Int. J. Hyperthermia*, **23**, 2007, pp. 315-323.

25. B. Hildebrandt, D. Schoeler, F. Ringel, T. Kerner, P. Wust, H. Riess, and F. Schriever, "Differential Gene Expression in Peripheral Blood Lymphocytes of Cancer Patients Treated with Whole Body Hyperthermia and Chemotherapy: A Pilot Study," *Int. J. Hyperthermia*, **22**, 2006, pp. 625-635.

26. A. Jordan and K. Maier-Hauff, "Magnetic Nanoparticles for Intracranial Thermotherapy," *J. Nanosci. Nanotechnol.*, **7**, 2007, pp. 4604-4606.

27. P. Wust, U. Gneveckow, M. Johannsen, D. Böhmer, T. Henkel, F. Kahmann, J. Sehouli, R. Felix, J. Ricke, and A. Jordan, "Magnetic Nanoparticles for Interstitial Thermotherapy – Feasibility, Tolerance and Achieved Temperatures," *Int. J. Hyperthermia*, **22**, 2006, pp. 673-685.

28. R. Hergt and S. Dutz, "Magnetic Particle Hyperthermia – Biophysical Limitations of a Visionary Tumour Therapy," *Journal of Magnetism and Magnetic Materials*, **311**, 2007, pp. 187-192.

29. G. Bellizzi and O. M. Bucci, "On the Optimal Choice of Exposure Conditions and Nanoparticles Features in Magnetic NanoParticles Hyperthermia," *Int. J. Hyperthermia*, **26**, 4, 2010, pp. 389-403.

30. F. Gazeau', M. Lévy, and C. Wilhelm, "Optimizing Magnetic Nanoparticle Design for Nanothermotherapy," *Nanomedicine*, **3**, 2008, pp. 831-844.

31. D. Faivre and D. Schler, "Magnetotactic Bacteria and Magnetosomes," *Chemical Reviews*, **108**, 11, 2008, pp. 4875-4898.

32. I. Safarik and M. Safarikova, "Magnetically Modified Microbial Cells: A New Type of Magnetic Adsorbents," *China Particuology*, **5**, 1-2, Magnetic Particulate Systems, 2007, pp. 19-25.

33. H. Fischer, G. Mastrogiacomo, J. F. Loffler, R. J. Warthmann, P. G. Weidler, and A. U. Gehring, "Ferromagnetic Resonance and Magnetic Characteristics of Intact Magnetosome Chains in Magnetospirillum Gryphiswaldense," *Earth and Planetary Science Letters*, **270**, 3-4, 2008, pp. 200-208.

34. R. Eelkema, M. M. Pollard, J. Vicario, N. Katsonis, B. S. Ramon, C. W. Bastiaansen, D. J. Broer, and B. L. Feringa, "Molecular Machines: Nanomotor Rotates Microscale Objects," *Nature*, March 9, 2006, 440(7081):163.

35. Y. Shirai, A. J. Osgood, Y. Zhao, K. F. Kelly, and J. M. Tour, "Directional Control in Thermally Driven Single-Molecule Nanocars," *Nano Lett.*, **5**, 11, 2005, pp. 2330-1334.

36. G. Vives and J. M. Tour, "Synthesis of Single-Molecule Nanocars," *Acc. Chem. Res.*, **42**, 3, 2009, pp. 473-487.

37. M. Endo and H. Sugiyama, "Chemical Approaches to DNA Nanotechnology," *Chembiochem.*, **10**, 15, 2009, pp. 2420-43.

38. G. Bellizzi, O. M. Bucci, and A. Capozzoli, "On the Energy Transfer Between the Electromagnetic Field and Nanomachines for Biological Applications," *Bioelectromagnetics*, **29**, 5, 2008, pp. 331-339.

39. P. Keblinski, D. G. Cahill, A. Bodapati, C. R. Sullivan, and T. A. Taton, "Limits of Localized Heating by Electromagnetically Excited Nanoparticles," *J. Appl. Phys*, **100**, September 2006, pp. 054305-1 – 054305-5.

40. R. K. Adair, "Vibrational Resonances in Biological Systems at Microwave Frequencies," *Biophys. J.*, **82**, 3, 2002, pp. 1147-1152.

41, G. Bellizzi, E. M. Bucci, and O. M. Bucci, "Analysis and Design of Magnetically Driven Nanomachines," *IEEE Transactions on Nanotechnology*, **10**, 5, 2011, pp. 1131-1140.

42. A. Noy, D. V. Vezenov, J. F. Kayyem, T. J. Meade, and C. M. Lieber, "Stretching and Breaking Duplex DNA by Chemical Force Microscopy," *Chem. Biol.*, **4**, 7, 1997, pp. 519-527.

43. C. Gosse and V. Croquette, "Magnetic Tweezers: Micromanipulation and Force Measurement at the Molecular Level," *Biophys. J.*, **82**, 6, 2002, pp. 3314-3329.

44. K. C. Neuman, T. Lionnet and J.-F. Allemand, "Single-Molecule Micromanipulation Techniques," *Annu. Rev. Mater. Res*., **37**, 2007, pp. 33-67.

45. P. Vavassori, M. Gobbi, M. Donolato, M. Cantoni, R. Bertacco, V. Metlushko, and B. Ilic, "Magnetic Nanostructures for the Manipulation of Individual Nanoscale Particles in Liquid Environments," *Journal of Applied Physics*, **107**, 9, 2010, pp. 09B301-1 –09B301-5.

46. M. Suwa and H. Watarai, "Magnetoanalysis of Micro/Nanoparticles: A Review," *Analytica Chimica Acta*, **690**, 2, 2011, pp. 137-147.

47. R. Skomski, "Nanomagnetics," *J. Phys.: Condens. Matter*, **15**, 2003, pp. 841-896.

48. T. R. Strick, D. Bensimon, and V. Croquette, "Micro-Mechanical Measurement of the Torsional Modulus of DNA," *Genetica*, **106**, 1999, pp. 57-62.

49. B. B. Yellen, O. Hovorka, and G. Friedman "Arranging Matter by Magnetic Nanoparticle Assemblers," *Proc. Natl. Acad. Sci. USA*, **102**, 25, 2005, pp. 8860-8864.

50. H. Joon Park, J. T. McConnell, S. Boddohi, M. J. Kipper, and P. A. Johnson, "Synthesis and Characterization of Enzyme-Magnetic Nanoparticle Complexes: Effect of Size on Activity and Recovery," *Colloids and Surfaces B: Biointerfaces*, **83**, 2, 2011, pp. 198-203.

51. A. Sharma, You Qiang, J. Antony, D. Meyer, P. Kornacki, and A. Paszczynski, "Dramatic Increase in Stability and Longevity of Enzymes Attached to Monodispersive Iron Nanoparticles," *IEEE Transactions on Magnetics*, **43**, 6, 2007, pp. 2418-2420.

52. E. Dujardin, C. Peet, G. Stubbs, J. N. Culver, and S. Mann, "Organization of Metallic Nanoparticles Using Tobacco Mosaic Virus Templates," *Nano Letters*, **3**, 3, 2003, pp. 413-417.

53. M. J. Martínez-Pérez, R. de Miguel, C. Carbonera, M. Martínez-Júlvez, A. Lostao, C. Piquer, C. Gómez-Moreno, J. Bartolomé, and F. Luis, "Size-Dependent Properties of Magnetoferritin," *Nanotechnology*, **21**, 46, 2010, pp. 465707.

54. H. Huang, S. Delikanli, H. Zeng, D. M. Ferkey, and A. Pralle, "Remote Control of Ion Channels and Neurons through Magnetic-Field Heating of Nanoparticles," *Nat. Nanotechnol*., **5**, 8, 2010, pp. 602-606.

Radio-Frequency Radiation Safety and Health

Zhangwei Wang
James C. Lin

Partial-Body SAR Calculations in Magnetic-Resonance Image (MRI) Scanning Systems

1. Introduction

The benefits of magnetic-resonance imaging (MRI) have made it the radiological modality of choice for a great number of diagnostic procedures. Aside from some acute potential risks, such as those from aneurysm clips or certain metal objects in the patient's body or scanner environment, no adverse health effects have been associated with clinical MRI. To form images, radio-frequency (RF) magnetic fields are used to excite and detect magnetic-resonance (MR) signals from body tissues. For the common 1.5 tesla (T) and, increasingly, 3.0 T clinical MRI scanners, the associated RF frequencies for proton imaging at 1.5 T and 3.0 T are about 64 MHz and 128 MHz, respectively.

To ensure that the RF energy absorbed by human subjects during MRI does not produce any harmful health effects to the patient – including local thermal damage or whole-body thermoregulatory challenges – regulatory entities have set limits on the maximum local, partial-body, and whole-body specific absorption rates (SAR) of RF energy [1-3]. There are two basic methods that are commonly employed or recommended by manufacturers to determine SAR delivered by their scanners: the power method, and the calorimetry method [4]. In the power method of measuring whole-body SAR for a subject of a given mass, the total patient absorption is calculated by subtracting the reflected power and power lost to the coil from the forward power. For the calorimetric method, the increase in whole-body temperature over a given duration is measured. Partial-body SAR is estimated by a formula that accounts for the ratio between exposed partial-body mass and total-body mass. This curve-fitting routine is typically used by the MRI system as the SAR monitor in radiological-imaging facilities. SAR values are obtained by entering the height and mass for the patient, in each case.

In principle, the same ratio methods may be used to calculate local SAR in smaller masses of exposed tissue. However, numerical methods combined with anatomical models should provide more-realistic or dependable local SAR values. Although many authors have published numerical computations of SARs in anatomical models of the human body for MRI [5-8], there are few reports presenting comparisons between results derived from various methods of SAR calculation.

Note that several anatomical models of the human body, with spatial resolutions ranging from 1 mm to 4 mm, have been reported for computational simulations under a variety of scenarios. The objective of this study is to examine partial-body and local SARs through numerical

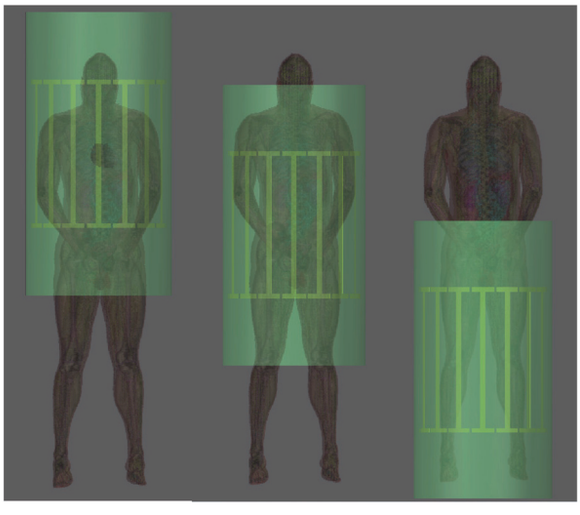

Figure 1. The geometry of the coil and the body model for partial-body SAR: (l-r) for coils centered on the chest, umbilicus, and knee regions, for partial-body exposure.

Zhangwei Wang is with GE Healthcare, 1515 Danner Drive, Aurora, OH 44202, USA. James C. Lin is with the Department of Electrical and Computer Engineering and Department of Bioengineering, University of Illinois at Chicago, 851 S. Morgan Street, MC 154, Chicago, IL 60607, USA; Tel: +1 (312) 413-1052; Fax: +1 (312) 996-6465; E-mail: lin@uic.edu.

[Essentially the same contribution appeared in the *IEEE Antennas and Propagation Magazine*, **54**, 2, April 2012, pp. 230-237; © 2012 IEEE.]

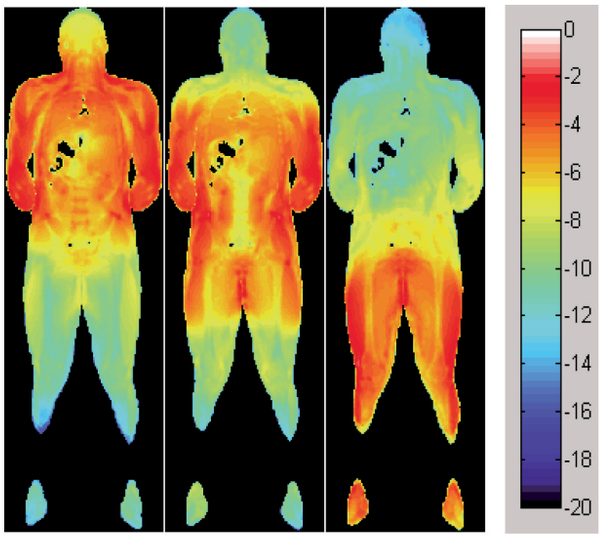

Figure 2a. The partial-body SAR distributions in coronal planes of the Visible Man in a birdcage MRI coil, for 1.5 T (1 g). From left to right are the partial-body SAR distributions for the chest, umbilicus, and knee coil positions, respectively. The data in the figure were normalized to one watt input power; a log scale was used.

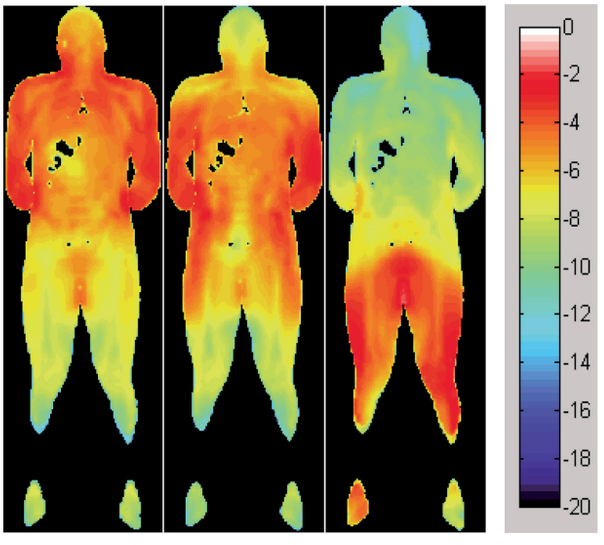

Figure 2b. The partial-body SAR distributions in coronal planes of the Visible Man in a birdcage MRI coil, for 3.0 T (10 g). From left to right are the partial-body SAR distributions for the chest, umbilicus, and knee coil positions, respectively. The data in the figure were normalized to one watt input power; a log scale was used.

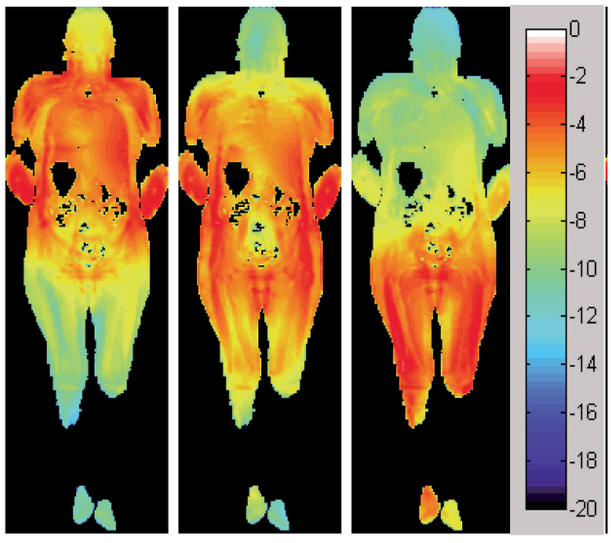

Figure 3a. The partial-body SAR distributions in coronal planes of the Visible Woman in a birdcage MRI coil, for 1.5 T (1 g). From left to right are the partial-body SAR distributions for the chest, umbilicus, and knee coil positions, respectively. The data in the figure were normalized to one watt input power; a log scale was used.

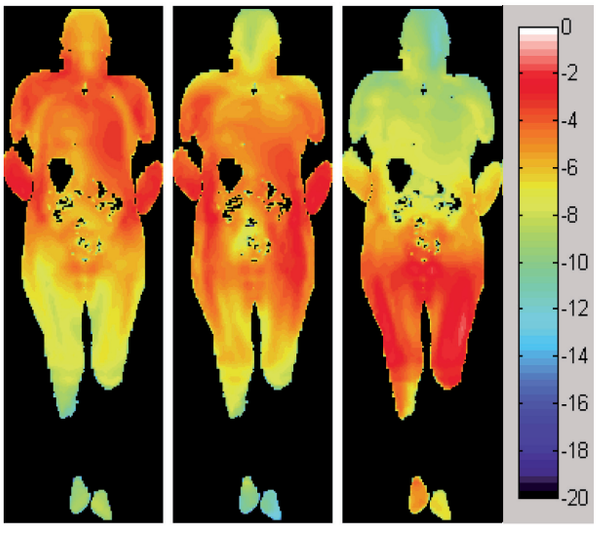

Figure 3b. The partial-body SAR distributions in coronal planes of the Visible Woman in a birdcage MRI coil, for 3.0 T (10 g). From left to right are the partial-body SAR distributions for the chest, umbilicus, and knee coil positions, respectively. The data in the figure were normalized to one watt input power; a log scale was used.

computations for anatomical models of male and female humans in 1.5 T (64 MHz) and 3.0 T (128 MHz) MRI systems. These are compared to results obtained from mass-ratio (curve-fitting) formulas used as SAR monitors in MRI scanners. In these computations, the birdcage coils were centered on the chest, umbilicus, and knee regions of the models for partial-body exposures.

2. Materials and Methods

The male and female human-body models from the Visible Human Project served as anatomical body models [9-11]. The Visible Man model consisted of 293 × 170 × 939 voxels, with 39 tissue types at a 2 mm isometric resolution. The Visible Woman model was interpolated to 266 × 143 × 864 voxels at 2 mm resolution. These models were adapted for the commercially available SEMCAD

Magnetic Flux Density (T)	1.5			3.0		
Coil Center Location	**Chest**	**Umbilicus**	**Knees**	**Chest**	**Umbilicus**	**Knees**
Mass in coil (kg)	52.20	60.43	23.99	52.20	60.43	23.99
Total power absorption (W)	0.91	0.91	0.75	0.98	0.98	0.99
Partial-body power absorption (W)	0.85	0.83	0.56	0.89	0.84	0.82
Whole-body average SAR (W/kg)	0.01	0.01	0.01	0.01	0.01	0.01
Partial-body average SAR (W/kg)	0.02	0.01	0.02	0.02	0.01	0.03

Table 1. The FDTD-computed absorbed powers and SARs for the Visible Man model at 1 W input power to the 1.5 T and 3.0 T birdcage coils (height: 1.876 m; mass: 105.64 kg).

finite-difference time-domain (FDTD) software (SPEAG, Zurich, Switzerland). The accuracy of the SEMCAD software was validated against published algorithms [12-13]. A four-parameter Cole-Cole extrapolation technique was used to determine values for the permittivity properties of various tissues [14-15].

A 16-rung, body-size high-pass birdcage coil was modeled (610 mm coil diameter and 620 mm length, with 660 mm shield diameter and 1220 mm length). For partial-body SAR calculations, the birdcage coils were centered on the chest, umbilicus, and knees of the human-body models (see Figure 1 for the model and coil). With the support of acceleration hardware (CIB 1000, SPEAG), the human models and the coil were meshed at in excess of 42 million voxels. The coils were driven with 32 current sources placed at the end-rings, and with a 22.5° phase shift between adjacent rungs. This scheme gave practically identical results as driving the coils at resonance in quadrature, for frequencies up to 128 MHz [16].

Local SARs in a body region surrounding a central voxel were averaged as the region was expanded by one voxel at a time until a specified mass of tissue (1 g, 10 g, partial body, or whole body) was reached. The International Electrotechnical Commission (IEC) scale was used to compute partial-body average SARs under the normal operating mode,

$$\mathrm{SAR} = 10\ \mathrm{W/kg} - \left(8\ \mathrm{W/kg} \frac{\text{exposed body mass}}{\text{total body mass}} \right), \quad (1)$$

and for the first-level controlled operating mode,

$$\mathrm{SAR} = 10\ \mathrm{W/kg} - \left(6\ \mathrm{W/kg} \frac{\text{exposed body mass}}{\text{total body mass}} \right). \quad (2)$$

3. Results

Partial-body SAR distributions in high-pass, birdcage MRI coils operating at 1.5 T (64 MHz) and 3.0 T (128 MHz) are shown in Figures 2 and 3 for the Visible Man and Woman models, respectively. It was interesting to note the similarity of the global pattern of SAR distributions. However, there were some differences for the two field strengths and human models. For example, the peak SAR values occurred in the skin (or surface) of the neck and shoulder for the chest coil position; at the skin of the arms and the abdomen for the umbilicus position; and for the knees, at the muscles of the knee joint and inner thigh areas for the knees, where the induced circulating RF currents were the highest.

The total and partial-body absorbed powers and SARs computed with the FDTD are given in Tables 1 and 2 for the Visible Man and Visible Woman, respectively, for 1 W input power to the 1.5 T and 3.0 T birdcage coils centered at the chest, umbilicus, and knees. As expected, the total power absorption was higher than the partial-body absorption. However, the whole-body average SARs were lower than those for partial-body locations at the chest, umbilicus, and the knees. Moreover, in general, power absorption at 3.0 T was 5% to 40% higher than at 1.5 T for the Man model, while the power absorption values varied from 3% to 50% for the Woman model at the same input power level. It was interesting to note that the total and partial-body power absorption values at 1.5 T were higher for the Man than for the Woman model, whereas the situation was reversed at 3.0 T.

Magnetic Flux Density (T)	1.5			3.0		
Coil Center Location	**Chest**	**Umbilicus**	**Knees**	**Chest**	**Umbilicus**	**Knees**
Mass in coil (kg)	45.97	50.33	19.80	45.97	50.33	19.80
Total power absorption (W)	0.87	0.97	0.69	1.00	1.00	1.00
Partial-body power absorption (W)	0.82	0.77	0.53	0.91	0.89	0.83
Whole-body average SAR (W/kg)	0.01	0.01	0.01	0.01	0.01	0.01
Partial-body average SAR (W/kg)	0.02	0.02	0.03	0.02	0.02	0.04

Table 2. The FDTD-computed absorbed powers and SARs for the Visible Woman model at 1 W input power to the 1.5 T and 3.0 T birdcage coils (height: 1.725 m; mass: 83.80 kg).

	Man Model			Woman Model		
Partial-body average SAR	**Chest**	**Umbilicus**	**Knees**	**Chest**	**Umbilicus**	**Knees**
Normal-mode operation (W/kg)	6.05	5.43	8.18	5.56	5.14	8.09
First-level control (W/kg)	7.05	6.57	8.64	5.67	6.35	8.57

Table 3. The partial-body average SAR limits calculated from IEC formulas for 1.5 T and 3.0 T coils for the Visible Man and Visible Woman models.

The IEC partial-body average SAR limits calculated from the above-mentioned formulas (Equations (1) and (2)) for both 1.5 T and 3.0 T coils and for the Visible Man and Visible Woman models are given in Table 3. It could be seen that the IEC formulas for the partial-body average SAR limits were higher for the Man model than for the Woman model, because of differences in body mass.

4. Discussion

It was observed that the IEC formulas (Equations (1) and (2)) for deriving the partial-body average SAR, and their use in specifying the partial-body average SAR limits (see Table 3), are based on body mass. They are not related to specific power absorption in specific tissues of the chest, umbilicus, or body extremities. Therefore, it was of interest to compare the IEC partial-body average SAR limits to those provided by FDTD calculations inside anatomical body models.

To illustrate the difference, the partial-body absorbed powers could be computed from multiplying the IEC limit (Equation (1)) by the appropriate mass. Under normal-mode operation, the computed partial-body absorbed powers for 1.5 T were 315.65 W, 327.75 W, and 196.32 W for the Man model, and 255.56 W, 258.55 W, and 160.13 W for the Woman model, for the chest, umbilicus, and knee positions, respectively. When these numbers were combined with the FDTD-calculated SARs given in Tables 1 and 2, they yielded the FDTD-computed partial-body SAR listed in Table 4, which corresponded to the powers permitted by the IEC limit for partial-body average SAR. It was noted that the IEC limit values were always higher than the FDTD computations. The IEC limits could be as high as 200%, and were about 130% higher on average, than the FDTD-computed SARs for both anatomical body models inside the MRI coil.

The peak local FDTD-calculated SAR values the IEC limits would allow could be found from the partial-body or whole-body average SAR using the formula

$$\mathrm{SAR}_{lp} = \left[\frac{\mathrm{SAR}_{IEC}}{\mathrm{SAR}_{FDTD}}\right]\left(\mathrm{SAR}_{FTDTD1\,g} \text{ or } \mathrm{SAR}_{FDTD10\,g}\right) \tag{3}$$

where SAR_{lp} is the peak local FDTD-calculated SAR values allowed by the IEC, SAR_{IEC} is the IEC SAR limit, SAR_{FDTD} is the FDTD-calculated whole-body average SAR at 1 W input power, and $\mathrm{SAR}_{FDTD1\,g}$ and $\mathrm{SAR}_{FDTD10\,g}$ are the FDTD-calculated peak SAR values for 1 g mass and 10 g mass, respectively, at 1 W input power. The peak SARs normalized to the IEC whole-body and partial-body average SAR limits calculated from the IEC formulas and the FDTD algorithm for 1.5 T and 3.0 T coils centered at the three body locations of the Visible Man and Visible Woman models are given in Tables 5 and 6, respectively, for the chest, umbilicus, and knee positions of the MRI coil.

Magnetic Flux Density (T)	**1.5**			**3.0**		
Coil Center Location	**Chest**	**Umbilicus**	**Knees**	**Chest**	**Umbilicus**	**Knees**
IEC partial-body absorbed power (W)	315.65	327.75	196.32	315.65	327.75	196.32
IEC partial-body average SAR (W/kg)	6.05	5.43	8.18	6.05	5.43	8.18
FDTD partial-body average SAR (W/kg)	5.15	4.46	4.60	5.37	4.52	6.71
IEC/FDTD partial-body average SAR ratio	1.18	1.22	1.78	1.04	1.14	1.21

Table 4a. The FDTD partial-body average SAR compared with limits calculated from IEC formulas for 1.5 T and 3.0 T coils for the Visible Man model.

Magnetic Flux Density (T)	**1.5**			**3.0**		
Coil Center Location	**Chest**	**Umbilicus**	**Knees**	**Chest**	**Umbilicus**	**Knees**
IEC partial-body absorbed power (W)	255.56	258.55	160.13	255.56	258.55	160.13
IEC partial-body average SAR (W/kg)	5.56	5.14	8.09	5.56	5.14	8.09
FDTD partial-body average SAR (W/kg)	4.55	3.96	4.26	5.09	4.55	6.74
IEC/FDTD partial-body SAR ratio	1.33	1.37	2.07	1.09	1.13	1.20

Table 4b. The FDTD partial-body average SAR compared with limits calculated from IEC formulas for 1.5 T and 3.0 T coils for the Visible Woman model.

	Chest		Umbilicus		Knees	
	SAR_1	SAR_{10}	SAR_1	SAR_{10}	SAR_1	SAR_{10}
Whole-body 2 W/kg (normal mode operation)	67.55	32.66	141.41	53.32	84.72	67.78
Whole-body 4 W/kg (first level control)	135.30	65.32	282.81	106.63	169.44	135.55
Partial-body SAR (normal mode operation)	107.75	52.02	243.35	91.76	104.87	83.90
Partial-body SAR (first level control)	125.35	60.52	294.69	111.11	110.69	88.56

* SAR_1 and SAR_{10} based on 1 g and 10 g of averaging tissue mass, respectively.

Table 5a. The peak local SARs (W/kg) normalized to the IEC whole-body and partial-body average SAR limits calculated from IEC formulas and FDTD algorithm for the 1.5 T coil centered at three body locations of the Visible Man model.*

	Chest		Umbilicus		Knees	
	SAR_1	SAR_{10}	SAR_1	SAR_{10}	SAR_1	SAR_{10}
Whole-body 2 W/kg (normal mode operation)	64.88	36.76	88.93	34.71	130.65	91.25
Whole-body 4 W/kg (first level control)	129.76	73.53	177.86	69.41	261.30	182.50
Partial-body SAR (normal mode operation)	106.99	60.63	160.99	62.82	150.60	105.18
Partial-body SAR (first level control)	124.47	70.53	194.95	76.08	158.96	111.02

* SAR_1 and SAR_{10} based on 1 g and 10 g of averaging tissue mass, respectively.

Table 5b. The peak local SARs (W/kg) normalized to the IEC whole-body and partial-body average SAR limits calculated from IEC formulas and FDTD algorithm for the 3.0 T coil centered at three body locations of the Visible Man model.*

The IEC local SAR limits for the head, trunk, and extremities are 10 W/kg, 10 W/kg, and 20 W/kg, respectively, for both normal and first-level controlled-operation modes. As can be seen from Tables 5 and 6, the peak local SARs were lower than the FDTD-computed SARs by a large margin in all cases. This implied that the IEC-permissible peak local SARs for the chest, umbilicus, and lower extremities could exceed the limit values of 10 W/kg and 20 W/kg by an average of threefold to six-fold, and by as much as 10-fold in both male and female patients under the normal operating mode, according to the Visible Man and Visible Woman models.

More specifically, the FDTD-calculated average local peak partial-body 1 g and 10 g SARs were 124.94 W/kg and 63.57 W/kg for the Man model, and 133.32 W/kg and 64.43 W/kg for the Woman model, respectively, at 1.5 T. Similarly, the FDTD 1 g and 10 g SARs were 117.17 W/kg and 65.20 W/kg for the Man model, and 112.86 W/kg and 62.52 W/kg for the Woman model, respectively, at 3.0 T. In addition to the above observation of a factor of three to six times higher than the IEC limits, a clear trend was also seen for the 1-g-based local peak SARs, which were twice as high as SAR values based on 10 g of equivalent mass.

In conclusion, the results showed that in both the 1.5 T and 3.0 T birdcage MRI coils, the FDTD-computed partial-body SARs were higher than the values given by the curve-fitting formulas for male and female patients. The local peak SARs allowed were considerably greater

	Chest		Umbilicus		Knees	
	SAR_1	SAR_{10}	SAR_1	SAR_{10}	SAR_1	SAR_{10}
Whole-body 2 W/kg (normal mode operation)	47.76	31.47	134.14	37.90	133.94	87.83
Whole-body 4 W/kg (first level control)	95.93	62.95	268.29	75.81	267.87	155.66
Partial-body SAR (normal mode operation)	78.40	51.66	236.53	66.83	169.12	110.90
Partial-body SAR (first level control)	94.06	61.98	292.51	82.65	179.12	117.46

* SAR_1 and SAR_{10} based on 1 g and 10 g of averaging tissue mass, respectively.

Table 6a. The peak local SARs (W/kg) normalized to the IEC whole-body and partial-body average SAR limits calculated from IEC formulas and FDTD algorithm for the 1.5 T coil centered at three body locations of the Visible Woman model.*

	Chest		Umbilicus		Knees	
	SAR_1	SAR_{10}	SAR_1	SAR_{10}	SAR_1	SAR_{10}
Whole-body 2 W/kg (normal mode operation)	46.58	31.08	108.61	42.08	111.43	77.98
Whole-body 4 W/kg (first level control)	93.16	62.15	217.22	84.16	222.86	155.96
Partial-body SAR (normal mode operation)	78.46	52.34	194.41	75.32	137.67	96.34
Partial-body SAR (first level control)	94.12	62.80	240.42	93.14	145.82	102.04

* SAR_1 and SAR_{10} based on 1 g and 10 g of averaging tissue mass, respectively.

Table 6b. The peak local SARs (W/kg) normalized to the IEC whole-body and partial-body average SAR limits calculated from IEC formulas and FDTD algorithm for the 3.0 T coil centered at three body locations of the Visible Woman model.*

than those specified in the IEC and FDA regulatory limits for both whole-body and partial-body SARs.

5. References

1. International Electrotechnical Commission (IEC).2010 International Standard, Medical Electrical Equipment Part 2-33: "Particular Requirements for the Basic Safety and Essential Performance of Magnetic Resonance Equipment for Medical Diagnosis," Geneva, IEC60601-2-33, edition 3.0.

2. Center for Devices and Radiologic Health (CDRH), "Guidance for the Submission of Premarket Notifications for Magnetic Resonance Diagnostic Devices," Rockville, MD, Food and Drug Administration, 1998; http://www.fda.gov/ cdrh/ode/ guidance/793.html.

3. J. C. Lin, "International Guidelines for Radio-Frequency Exposure, Especially for the Most Successful Application of Electromagnetics in Medicine: Magnetic Resonance Imaging," *IEEE Antennas and Propagation Magazine*, **53**, 1, February 2011, pp. 169-174.

4. National Electrical Manufacturers Association (NEMA), "1903 Characterization of SAR for MRI Systems," Rosslyn, VA, USA NEMA Standard MS-8-1993.

5. C. M. Collins and M. B. Smith, "Spatial Resolution of Numerical Models of Man and Calculated Specific Absorption Rate Using the FDTD Method: A Study at 64 MHz in a Magnetic Resonance Imaging Coil," *Journal of Magnetic Resonance Imaging*, **18**, 2003, pp. 383-388.

6. C. M. Collins, W. Z. Liu, J. H. Wang, W. Gruetter, J. T. Vaughan, K. Ugurbil, and M. B. Smith, "Temperature and SAR Calculations for a Human Head Within Volume and Surface Coils at 64 and 300 MHz," *Journal of Magnetic Resonance Imaging*, **19**, 2004, pp. 650-656.

7. Z. W. Wang, J. C. Lin, W. H. Mao, et al., "SAR and Temperature: Calculations and Comparison to Regulatory Limits for MRI," *Journal of Magnetic Resonance Imaging*, **26**, 2007, pp. 437-441.

8. T. S. Ibrahim and L. Tang, "Insight into RF Power Requirements and B_1 Field Homogeneity for Human MRI via Rigorous FDTD Approach," *Journal of Magnetic Resonance Imaging*, **25**, 2007, 1235-1247.

9. Z. W. Wang, J. C. Lin, J. T. Vaughan, and C. M. Collins, On Consideration of Physiological Response in Numerical Models of Temperature During MRI of the Human Head," *Journal of Magnetic Resonance Imaging*, **28**, 2008, pp. 1303-1308.

10. C. M. Collins and Z. W. Wang, "Calculation of Radiofrequency Electromagnetic Fields and their Effects in MRI of Human Subjects," *Magnetic Resonance in Medicine*, **65**, 2011, pp. 1470-1482.

11. D. T. B. Yeo, Z. W. Wang, W. Loew, et al., "Local Specific Absorption Rate in High-Pass Birdcage and Transverse Electromagnetic Body Coils for Multiple Human Body Models in Clinical Landmark Positions at 3T," *Journal of Magnetic Resonance Imaging*, **33**, 2011, pp. 1209-1217.

12. Z. W. Wang, C. W. Penney, R. J. Luebbers, and C. M. Collins, "Poseable Male and Female Numerical Body Models for Field Calculations in MRI," Proceedings of the 16th Annual Meeting ISMRM, Toronto, Canada, 2008.

13. J. C. Lin and Z. W. Wang, "Acoustic Pressure Waves Induced in Human Heads by RF Pulses from High-Field MRI Scanners," *Health Physics*, **98**, 2010, pp. 603-613.

14. C. Gabriel, "Dielectric Properties of Biological Tissue: Variation with Age," *Bioelectromagnetics*, **26**, 2005, pp. S12-S18.

15. S. Gabriel, C. Gabriel, and R. W. Lau, "The Dielectric Properties of Biological Tissues: III. Parametric Models for the Dielectric Spectrum of Tissues," *Phys. Med. Biol.*, **41**, 1996, pp. 2271-2293.

16. W. Liu, C. M. Collins, and M. B. Smith, "Calculations of B1 Distribution, Specific Energy Absorption Rate, and Intrinsic Signal-to-Noise Ratio for a Body-Size Birdcage Coil Loaded with Different Human Subjects at 64 and 128 MHz," *Appl. Magn. Reson.*, **29**, 2005, pp. 5-18.

Book Reviews for Radioscientists

[Editor's note: The Young Scientists who received an award at the 2011 Istanbul URSI GASS were asked to review their favorite textbook, even if it was a classic book. This is in contrast to our usual reviews, where we try to have new books reviewed. The reviews in this issue are from Young Scientists.]

Antennas and Wave Propagation

By John D Kraus, Ronald J. Marhefka, and Ahmad S. Khan, New York, McGraw Hill, 2011; ISBN 0-07-067155-9.

"Antennas," the eyes to the wireless world, are highly complicated and challenging. The research on antennas began many decades ago, but there still remains a lot to pursue. The emergence of new wireless applications makes antennas the hottest area of research among the electromagnetics community. Understanding this field clearly and truthfully is the primary step for RF and microwave scientists and students, and can be easily achieved through this book.

The authors of the book are J. D. Kraus, Ronald J. Marhefka, and Ahmad S. Khan. The majority of the chapters in this book have been derived by modifying their earlier editions, and by adding four new chapters on wave propagation on the basics of wave propagation, and ground-wave, space-wave, and sky-wave propagation. Chapters exclusively on radiation and microstrip antennas are also included, with extensive coverage of the newest wireless applications. The book consists of 25 chapters and one appendix, covering nearly 900 pages. I felt that the authors have taken great care to allow readers to bridge the gap between theory and experiment by providing nearly 130 worked examples, found at the end of each chapter.

Different sections of this book have been contributed partly or fully by professors who are experts in the area. Prof. Ben A. Munk from Ohio State University contributed to frequency-selective surfaces, periodic structures, and baluns. The chapters on antenna measurements were comprehensively discussed by professors from Helsinki University: Arto Lehto and Perttl Valnlkalnen. Prof. Edward H. Newman of Ohio State University explained self impedance, RCS, and the mutual impedance of short dipoles by the Method of Moments. Christopher Walker, a Professor of Astronomy from the University of Arizona, contributed to the terahertz lens and waveguide structures. Prof. Pertti Vainikainen contributed to antennas for terrestrial mobile communication systems. Not only is the book a useful teaching resource, but it is highly informative for antenna researchers and scientists.

The first three chapters provide some fundamental information to the reader. A short history of antenna basics, including radiation phenomena, signal-to-noise ratio, antenna temperature, antenna impedance and front-to-back ratio, is provided. Moreover, various types of antennas are also briefly described, with antenna theorems and a table of antenna parameters. The next two chapters are devoted to radiation phenomena, point sources, and arrays. The mathematical theory related to antennas, with a discussion of the retarded potential and the far field due to alternating and sinusoidal current distributions, is also discussed. This material describes point sources and their fields, power and phase patterns, together with the formation of arrays, leading the reader to acquire knowledge about broadside and end-fire arrays of point sources.

The next two chapters give information about basic antennas, such as linear, loop, slot, and horn antennas. Dipole and linear antennas are also discussed, alone and in arrays. The axial-mode helical antenna and Yagi-Uda arrays are included in Chapter 8. The concept of the helix mode is introduced in this chapter. Reflector antennas, with a clear illustration of feed arrangements together with an explanation of lens antennas and similar types, are given in Chapter 9 and Chapter 10. Rumsey's principle for frequency-independent antennas is discussed in Chapter 11 ("Broadband and Frequency-Independent Antennas"). The Moment Method is explained with an application to wire antennas, together with cylindrical antennas, in Chapter 12. An introduction to frequency-selective surfaces and periodic structures is given in Chapter 13. Radomes, which are used extensively in various electromagnetic applications, are discussed.

The basic microstrip antenna is explained in Chapter 14. This is followed by antennas for special applications in Chapter 15, such as cell-phone antennas, instrument-landing-system antennas, and low-Earth-orbit satellite antennas. The important practical design considerations required when designing large-aperture antennas are explained in Chapter 16. The following chapter discusses antenna temperature, remote sensing, and radar cross section. The impedance of an antenna is an important factor that determines the antenna's radiation characteristics. The mutual impedance between two parallel antennas and the self impedance of thin linear antennas are discussed in Chapter 18. It is very important to know how the far-field pattern of an antenna is obtained from knowledge of the aperture distribution. This topic is discussed in detail in this chapter. Moreover, the spatial-frequency response, pattern smoothing, and a simple interferometer are aptly discussed.

Balanced-to-unbalanced transformers are discussed in the next chapter, with a complete up-to-date discussion of antenna measurements in Chapter 21. The last four chapters are completely devoted to wave propagation, starting from the basics of wave propagation towards the ground, space, and the sky.

This book can be recommended for students, researchers, and professionals who either want to learn about or are actively working in the field of antennas and propagation. It provides a good starting point for those new to the topic, while at the same time being a good reference source for engineers and researchers working in the area.

Reviewed by:
Sujith Raman
WiSAR Lab, Letterkenny Institute of Technology
Letterkenny, County Donegal, Ireland
E-mail: sujithrpkd@gmail.com

Mobile Communications Design Fundamentals, Second Edition

By William C. Y. Lee, New York, John Wiley & Sons, 1993, 372+xix pp.; ISBN: 0-471-57446-5

It is a great honor for me to review the book *Mobile Communications Design Fundamentals, Second Edition*" by William C. Y. Lee. Despite the lapse of time after its publication, this book describes many current aspects of the design of mobile-radio systems.

Prof. William C. Y. Lee, the author of the reviewed book, is commonly recognized as an authority on wireless communication. He took part in developing a number of advanced wireless-technology solutions, e.g., AMPS for Bell Labs and the first commercial CDMA system. He is also an author of a UHF propagation model, the very-well-known Lee Model. A list of his achievements and memberships in prestigious communities and organizations is very long and impressive. However, in this review I will focus on his book, which should be known to every radio scientist, especially the young.

In general, the book concerns the design of mobile radio systems. It provides answers for the main questions that appear while planning such systems.

Chapter 1 deals with the basics of the mobile radio environment, describing such issues as mobile radio signal representation, definitions and applications of necessary terms, and the reciprocity principle. The causes of propagation path loss and fading are also described.

Chapter 2 is devoted in its entirety to the prediction of propagation loss. At the beginning, the author points out that the best way to predict the basic transmission loss is a combination of statistics and electromagnetic theory. Due to the statistics, there is very important practical advice on how to obtain meaningful path-loss data from measurements. Afterwards, there is a wide description of the prediction methodology for various conditions, such as flat terrain, unobstructed or obstructed conditions, microcells, and even tunnels.

Chapter 3 focuses on the calculation of various types of fades and methods for reducing this phenomena, using diversity schemes and combining techniques. These schemes and techniques are the methods for creating the least correlation between two fading signals received by more than one input of the mobile receiver. This chapter describes the bit-error rate and word-error rate in such environments, as well.

Chapter 4 is related to the interference that occurs in mobile-radio communication. The co-channel and adjacent-channel interference are described, as well as the inter-symbol or simulcast interference. There are also characteristics of intermodulation and the so-called near-far effect discussed.

In order to reduce adjacent-channel interference or intermodulation, and to maximize the spectrum utilization as well, a proper frequency plan is needed. This subject is taken up in Chapter 5, where the frequency plans and their associated schemes (e.g., FDM or TDM) are described.

The next two chapters include practical guidelines that are useful when designing the parameters of a base station (Chapter 6) and a mobile unit (Chapter 7). These guidelines take into account all the important parameters of the considered radio link and the environmental conditions. The main accent is put on the antenna, its location, spacing, height, and configuration. There is also a description of the noise environment, and some advice regarding power and field-strength conversions. For the case of a mobile unit, whether it stands still or is in motion is important.

Chapter 8 deals with signaling and channel access. The chapter takes up such subjects as the criteria for signaling design, channel assignment, switching capacity, and word-error rate in various environments (e.g., Gaussian or Rayleigh fading).

Chapter 9 is devoted in whole to the code division multiple access (CDMA) scheme as a technique mainly for increasing the capacity of cellular systems. After answering the question, "Why CDMA?," the author describes

narrowband and wideband wave propagation. Afterwards, he mentions key elements of designing cellular systems, spreading techniques in modulation, and the capacities of multiple-access schemes. There is also one paragraph about the reduction of near-far-ratio interference in CDMA.

Chapter 10 is related to microcell systems. First, the author describes the design of a conventional cellular system. Afterwards, a description of the design of new microcell systems is presented. The author also analyses the capacity and voice quality in such systems, and a problem of the reduction of hand-offs.

The last chapter concerns the characteristics of miscellaneous related systems with respect to mobile systems described in the previous chapters. The author considers the following systems: the personal communication service (PCS), portable telephone systems, systems for air-to-ground communications, and systems for land-mobile and satellite communication.

To sum up, the reviewed book is very worthwhile for everyone who is interested in designing mobile radio systems. Because each chapter ends with problems concerning the issues raised, this book is especially destined for teachers and their students as an excellent source of knowledge.

Reviewed by:
Slawomir J. Ambroziak
Dept. of Radiocomm. Systems & Networks
Fac. of Electronics, Telecomm. &Informatics
Gdansk University of Technology
11/12 Narutowicza Street, 80-233 Gdansk, Poland
E-mail: sj_ambroziak@eti.pg.gda.pl

Conferences

URSI CONFERENCE CALENDAR

An up-to-date version of this conference calendar, with links to various conference web sites can be found at http://www.ursi.org/en/events.asp

August 2012

ICTRS 2012 - First International Conference on Telecommunications and Remote Sensing
Sofia, Bulgaria, 29-31 August 2012
Contact: Prof. Blagovest Shishkov, Institute of Mathematics and Informatics at Bulgarian Academy of Sciences, 1113 Sofia, Bulgaria, Fax :+359 2 971 3649, E-mail: bshishkov@math.bas.bg

September 2012

ICEAA 2012 - International Conference on Electromagnetics in Advanced Applications
Cape Town, South Africa, 2-8 September 2012
Contact: ICEAA - IEEE 2012 Conference, Consult US (Pty) Ltd, PO Box 19063, Tygerberg, 750, Fax +27 21 933 2649, E-mail: iceaa12@iceaa.polito.it

VERSIM Workshop
Sao Paulo, Brazil, 2-8 September 2012
Contact: Prof. F.C.P. Bertoni, CRAAM/EE/UPM, Rue da Consolaçao 896 Prédio T, 7 andar, CEP 01302-907 Sao Paulo, SP, Brazil

EMC Europe 2012 -International Symposium on Electromagnetical Compatibility
Rome, Italy, 17-21 September 2012
Contact : Marcello D Amore, Department of Electrical Engineering, Sapienza University of Rome, Rome, Italy Via Eudossiana 18, I-00184 Rome, Italy, E-mail : marcello.damore@uniroma1.it, website, http://www.emceurope2012.it

Metamaterials 2012
St. Petersburg, Russia, 17-22 September 2012
E-mail : contact@congress2012.metamorphose-vi.org

RADIO 2012 - Radio and Antenna Days of the Indian Ocean
Mauritius, 24-27 September 2012
Contact: Vikass Monebhurrun, Dept of Electromagnetics, DRE-L2S, SUPELEC, 3, Rue Joliot-Curie, 91192 Gif-sur-Yvette Cedex, France, Fax +33 1 69851569, E-mail vikass.monebhurrun@supelec.fr

October 2012

ISSSE 2012 - International Symposium on Signals Systems and Electronics
Potsdam, Germany, 3-5 October 2012
Prof. Rolf Kraemer, IHP GmbH, Dept. System Design, Im Technologiepark 25, 15236 Frankfurt (O), Germany, E-mail: Kraemer@ihp-microelectronics.com

November 2012

ISAP 2012 - 2012 International Symposium on Antennas and Propagation
Nagoya, Japan, 29 October - 2 November 2012
Professor Koichi Ito, General Chair of ISAP2012, Chiba University, 1-33 Yayoi-cho, Inage-ku, Chiba-shi, Chiba 263-8522, Japan, Fax: +81-43-290-3327, E-mail: ito.koichi@faculty.chiba-u.jp

RFID-Technology and Applications 2012
Nice, France, 5-7 November 2012
Contact: Smail TEDJINI, General Chair of IEEE RFID-TA 2012, NPG-ESISAR, LCIS, 50, rue B. de Laffemas, BP 54, F-26902 VALENCE CEDEX 9, FRANCE, Fax +33 4 75 43 5642

December 2012

ICMARS 2012 - International Conference on Microwaves, Antenna Propagation & Remote Sensing
Jodhpur, India, 11-15 December 2012
Contact : Prof. O.P.N. Calla, International Centre for Radio Science, Plot No1, Rano ji Ka Bagh, Khokhariya Bera, Nayapura, Mandore, Jodhpur 342304 Rajasthan, India, Tel +91 291 2571030, Fax +91 291 257 1390

April 2013

EUCAP 2013
Gothenburg, Sweden, 8-12 April 2013
Contact: Prof. G. Kristensson, Dept. Electrical & Information Technology, P.O. Box 118, S2-221 Lund; Sweden, E-mail Gerhard.Kristenssoneit.lth.se

July 2013

Beacon Satellite Meeting
Bath, Uk, 8-12 July 2013
Contact: Ms. Patrica Doherty, Boston University School of Management, 595 Commonwealth Avenue, Boston, MA 02215, USA, E-mail : pdoherty@bu.edu, Website : http://www.bc.edu/research/isr/ibss.html

September 2013

ICEAA-APWC-EMS conferences
Torino, Italy, 9-13 September 2013
Contacts: Prof. W.A. Davis, EMS Chair wadavis@vt.edu and Prof. Y. Koyama, EMS Vice-Chair koyama@nict.go.jp

URSI cannot be held responsible for any errors contained in this list of meetings

News from the URSI Community

NEWS FROM A MEMBER COMMITTEE

FRANCE

Prix étudiant de l'URSI 2012

Le Prix étudiant de l'URSI 2012 a été attribué à Pierre Jarrige pour l'article intitulé «Mesure dosimétrique par capteur électro-optique fibré » lors des Journées scientifiques d'URSI-France, «Champs électromagnétiques, de la dosimétrie à la santé humaine», tenues à Paris, les 3 et 4 avril dernier.

Pierre Jarrige est né en 1981 à Brive-la-Gaillarde. Il effectue actuellement son doctorat (2009-2012) au Laboratoire d'hyperfréquences et de caractérisation de l'institut de microélectronique électromagnétisme et photonique (IMEP-LAHC) dans le cadre d'une convention industrielle de formation par la recherche (CIFRE) faisant intervenir la société Kapteos ainsi que la Direction générale pour l'armement (DGA). Ses travaux, dirigés par Lionel Duvillaret et Gwenaël Gaborit, concernent le développement de capteurs électro-optiques dédiés à la mesure simultanée du champ électrique et de la température au sein des milieux biologiques pour des applications en bioélectromagnétisme (dosimétrie micro-onde ou encore électroporation cellulaire).

GERMANY

Kleinheubacher Tagung 2012

The 'Kleinheubacher Tagung 2012' of the German URSI Committee will be organised from 24. – 26. September 2012 in Miltenberg, Germany.

Topics

The topics are:
A: Electromagnetic Metrology
B: Fields and Waves
C: Radio Communication Systems and Signal Processing
D: Electronics and Photonics
E: Electromagnetic Environment and Interference
F: Wave Propagation and Remote Sensing
G: Ionospheric Radio and Propagation
H: Waves in Plasmas
J: Radio Astronomy
K: Electromagnetics in Biology and Medicine

Call for Papers

The organisers require the use of electronic submission through the website http://www.edas.info, before July 20, 2012. Please mention the Title, Author(s), one abstract (only text, not more than 500 words) and the Commission.

Contact

For more information, please visit the website http://meetings.copernicus.org/kh2012/ or contact ursi2012@hft.ei.tum.de

Important dates

20 July 2012: submission deadline
31 August 2012: registration deadline
24.-26. September 2012: Kleinheubacher Tagung 2012

Call for Papers

Radio Science Bulletin

Special Issue on the Role of Radio Science in Disaster Management

Between 1975 and 2009, 10,000 natural disasters in the world killed more than 2,500,000 people, with an amount of the damage totaling more than 1.7 trillion US dollars. The main causes were earthquakes, landslides, cyclones, storms, and floods, and infectious illness.

Science and technology can contribute to the reduction of the impact of these disasters. Radio science has a central role in the management of disasters. Radio science constitutes an essential component for supervising the environment, and for collecting data in order to feed forecasting models that have a large influence on the reliability of decision making. In the context of a significant destruction of infrastructure, radio communications become critical for the organization of rescue operations.

The objective of this special issue is to review contributions resulting from radio science in order to decrease the impact of such disasters, and to encourage the scientists to think of how they can contribute to reducing the impact of such events. The partial list below provides examples of the contributions of radio sciences

The main topics of interest include but are not limited to:

- Communication facilities for disaster management
- The use of radio techniques for disaster prediction
- Radio remote sensing for disaster detection, disaster management, and post-disaster programs
- All other topics related to the application of radio science to disaster prediction, detection, mitigation, management, and recovery

Guest Editors

Prof. Tullio Joseph Tanzi, Télécom ParisTech–LTCI/CNRS, Paris, France
Prof. François Lefeuvre, LPC2E/CNRS, URSI, Orléans, France
Prof. P. J. Wilkinson, IPS, Bureau of Meteorology, Australia

Papers must be written in English and describe original research not published or currently under review by other journals or conferences. Submissions should be sent in the format for the *Radio Science Bulletin* via e-mail to tullio.tanzi@telecom-ParisTech.fr.

Proposed schedule

Manuscript submission: **October 15th, 2012**
Expected publication: Second semester 2013

National Radio Science Meeting

◆ January 9-12, 2013 ◆ University of Colorado at Boulder
◆ Meeting website: www.nrsmboulder.org
◆ USNC-URSI website: www.usnc-ursi.org

This open scientific meeting is sponsored by the U.S. National Committee (USNC) of the International Union of Radio Science (URSI). The USNC-URSI is appointed by the National Research Council of The National Academies and represents U.S. radio scientists in URSI. The meeting is held in cooperation with the following IEEE organizations: Antennas and Propagation Society, Circuits and Systems Society, Communications Society, Electromagnetic Compatibility Society, Geoscience and Remote Sensing Society, Information Theory Society, Instrumentation and Measurement Society, Microwave Theory and Techniques Society, and Nuclear Science Society. Papers on any topic in the interest area of a Commission are welcome. Contact the Commission Chairperson or visit the website for further information.

Meeting Highlight: ***Remote Sensing and Communication Systems in Disaster Mitigation and Response***
Contacts: V. Chandrasekar (Comm. F Chair), chandra@engr.colostate.edu
Amir I. Zaghloul (Comm. C Chair), amirz@vt.edu

USNC-URSI Chair: Steven C. Reising, (970) 491-2228, Steven.Reising@ColoState.edu
USNC-URSI Secretary: David R. Jackson, (713) 743-4426, djackson@uh.edu

COMMISSION A, Electromagnetic Metrology

Christopher L. Holloway, (303) 497-6184, holloway@boulder.nist.gov

TOPICS

Antennas
Bioeffects and medical applications
EM-field metrology
EMC and EM pollution
Impulse radar
Interconnect and packaging
Materials
Microwave to submillimeter measurements/standards
Millimeter-wave and sub-mm wave communications
Noise
Planar structures and microstrip circuits
Quantum metrology and fundamental concepts
Time and frequency
Time domain metrology

COMMISSION B, Fields and Waves

Sembiam Rengarajan, (818) 677-3571, srengarajan@csun.edu

TOPICS

Antenna arrays
Antenna theory, design and measurements
Cognitive radio
Complex media (metamaterials, bandgap structures, biological and geophysical media, and others)
Educational methods and tools
Electromagnetic interaction and coupling
Guided waves and waveguiding structures
High-frequency techniques
Inverse scattering and remote sensing
Microstrip and printed devices and antennas
Nonlinear electromagnetics
Numerical methods (differential- and integral-equation based, hybrid and other techniques)
Propagation phenomena and effects
Rough surfaces and random media
Scattering
Theoretical electromagnetics
Transient fields, effects, and systems
Ultra-wideband electromagnetics
Wireless communications

COMMISSION C, Radio-communication Systems and Signal Processing

Amir I. Zaghloul, (703) 538-8435, amirz@vt.edu

TOPICS

Cognitive radio
Computational imaging and inverse methods
Distributed sensor networks
Physics-based signal processing
Radar target detection, localization, and tracking
Sensor array processing and calibration
Signal processing for radar remote sensing
Statistical signal processing of waves in random media
Synthetic aperture and space-time processing

COMMISSION D, Electronics and Photonics

Jennifer T. Bernhard, (217) 333-0293, jbernhar@illinois.edu

TOPICS

Electronic devices, circuits, and applications
Photonic devices, circuits, and applications
Physics, materials, CAD, technology and reliability of electronic and photonic devices, in radio science and telecommunications
Wide bandgap materials

Abstract submissions
and
Student Paper Competition submissions
are due by
September 21, 2012
These are FIRM DEADLINES!
Please visit *www.nrsmboulder.org*

COMMISSION E, Electromagnetic Environment and Interference

Everett G. Farr, (505) 293-3886, efarr@farr-research.com

TOPICS

Communication in the presence of noise
Effects of natural and intentional emissions on system performance
Electromagnetic compatibility in: computational electromagnetics, education, measurement technologies, standards, and radiation hazards
High-power electromagnetic effects of transients on electronic systems
Spectrum management and utilization

COMMISSION F, Wave Propagation and Remote Sensing

V. Chandrasekar, (970) 491-7981, chandra@engr.colostate.edu

TOPICS

Point-to-point propagation effects:

Measurements	*Mobile/fixed paths*
Propagation models	*Horizontal/slant paths*
Multipath/mitigation	*Surface/atmosphere interactions*
Land or water paths	*Atmospheric constituents*
Scattering/diffraction	*Dispersion/delay*
Indoor/outdoor links	*Natural/man-made structures*

Remote sensing of the Earth by radio waves:

Atmospheric sensing	*Ocean and ice sensing*
Field campaigns	*Interferometry and SAR*
Subsurface sensing	*Scattering/diffraction*
Radiation and emission	*Propagation effects*
Urban environments	*Soil moisture & terrain*

Propagation and remote sensing in complex and random media

COMMISSION G, Ionospheric Radio and Propagation

Frank Lind, (781) 981-5570, flind@haystack.mit.edu

TOPICS

Ionospheric imaging
Ionospheric morphology
Ionospheric modeling and data assimilation
Radar and radio techniques for ionospheric diagnostics
Space weather – radio effects
Transionospheric radio propagation and systems effects

COMMISSION H, Waves in Plasma

Victor Pasko, (814) 865-3467, vpasko@psu.edu

TOPICS

Chaos and turbulence in plasma
Plasma instabilities
Spacecraft-plasma interactions
Solar/planetary-plasma interactions
Space as a research laboratory
Wave-wave and wave-particle interactions
Waves in space and laboratory plasmas

COMMISSION J, Radio Astronomy

Richard F. Bradley, (434) 296-0291, rbradley@nrao.edu

TOPICS

Detection of short-duration transients
Developments in array technology for radio astronomy
New telescopes, techniques, and observations
Radio frequency interference mitigation and spectrum usage
Timely technical tutorials

COMMISSION K, Electromagnetics in Biology and Medicine

Erdem Topsakal, (662) 325-3669, topsakal@ece.msstate.edu

TOPICS

Biological effects
Dosimetry and exposure assessment
Electromagnetic imaging and sensing applications
Human body interactions with antennas and other electromagnetic devices
Therapeutic, rehabilitative and other biomedical applications

ERNEST K. SMITH USNC-URSI STUDENT PAPER COMPETITION

Prizes will be awarded to three graduate student papers. Awards will be made for First Prize in the amount of $1000, Second Prize at $750, and Third Prize at $500. The deadline for submission of ***full papers*** on the meeting website is ***September 21, 2012***. Please see *www.nrsmboulder.org* for additional information, or contact the Student Paper Chair Prof. Danilo Erricolo, Dept. of ECE, University of Illinois at Chicago, erricolo@ece.uic.edu. Student papers and awards will be presented at the Plenary Session on Thursday morning, January 10, 2013. Student Paper Competition participants will have the option of submitting their full papers for publication in a special section of the journal Radio Science.

ABSTRACT SUBMISSION

The organizers of this meeting require the use of electronic submission. Details and instructions may be found at *www.nrsmboulder.org*. All abstract submission information must be entered online by **Friday, September 21, 2012**. If you have any questions on abstract submission or the technical program, please direct them to USNC-URSI Secretary David R. Jackson at *djackson@uh.edu*. Abstracts must be a *minimum of 250 words*. You will not be able to submit an abstract that does not meet the minimum length requirements. After abstract submission is complete, please note that *registration is required* to attend any session of the meeting or to present a paper. More information about USNC-URSI is available at *www.usnc-ursi.org*.

Questions about the conference

For questions concerning logistics (including travel and lodging) and the conference program, please contact:
Christina Patarino, Phone: (303) 492-5151, Fax: (303) 492-5959, E-mail: christina.patarino@colorado.edu

URSI Commission B
2013 International Symposium on Electromagnetic Theory

Hiroshima, Japan May 20-24, 2013

www.ursi-emts2013.org

General Information

The "2013 International Symposium on Electromagnetic Theory" (EMTS 2013) is organized by Commission B (Fields and Waves) of the International Union of Radio Science (URSI) and the Electronics Society of The Institute of Electronics, Information and Communication Engineers (IEICE). It will be held on May 20-24, 2013 in Hiroshima, Japan. Its scope covers all areas of electromagnetic theory and its applications.

Important Dates

Nov. 1, 2012	Deadline for receipt of YSA papers
Nov. 15, 2012	Deadline for receipt of papers
Jan. 15, 2013	Notification of authors regarding acceptance of papers, notification of YSA applicants
Mar. 15, 2013	Deadline for pre-registration of authors(All presenting authors must pre-register)
April 30, 2013	Deadline for pre-registration of participants
May 20, 2013	URSI Commission B School for Young Scientists
May 20-24, 2013	Symposium

Young Scientist Awards

Young Scientist Awards (YSA) have been planned for young scientists. For details, visit the website.

Suggested Topics

Contributions concerning all aspects of electromagnetic theory and its applications are welcome. Novel and innovative contributions are particularly appreciated. Special topics will also be announced in the Final Call for Papers in addition to the following list.

- New basic theoretical developments
- Scattering and diffraction
- Inverse scattering and imaging
- Time domain methods
- High-frequency methods
- Guided waves
- Solutions to canonical problems
- Propagation and scattering in layered structures
- Random media and rough surfaces
- Metamaterials and complex media
- Beam and pulse propagation and scattering in lossy and/or dispersive media
- Non-linear phenomena
- Antennas: general aspects
- Antenna arrays, planar and conformal
- Numerical methods: general aspects
- Numerical methods for integral and differential equations
- Hybrid methods
- Interaction of EM waves with biological tissues
- EM theory and applications for radio systems
- Antennas and propagation for communication systems
- Smart antennas, UWB systems, etc.
- Mathematical modeling of EM problems

Submissions and Further Information

The instructions for the submission of papers and the updated information on the Symposium will be available in the Final Call for Papers and on the conference Web site. Copyrights of all accepted papers are to be transferred to the IEICE.

All accepted and presented papers will be available through IEEE Xplore.

URSI Commission B School for Young Scientists

The "URSI Commission B School for Young Scientists" will be organized for the first time at EMTS 2013 in Hiroshima. In this one-day school, a series of lectures will be delivered by leading scientists in the Commission B community and young scientists are encouraged to learn the fundamentals and future directions in the area of electromagnetic theory. Details will be announced later.

Conference Contacts

General questions and technical program:

Chair, Conference and Commission B of URSI

Prof. Giuliano Manara

Department of Information Engineering,

University of Pisa, Italy

E-mail: g.manara@iet.unipi.it

Questions regarding local arrangements:

Co-Chairs, Local Organizing Committee

Prof. Makoto Ando

Dept. of Electrical and Electronics Engineering

Tokyo Institute of Technology, Japan

E-mail: mando@antenna.ee.titech.ac.jp

Prof. Tsuneki Yamasaki

College of Science and Technology

Dept. of Electrical Engineering

Nihon University, Japan

E-mail: yamasaki@ele.cst.nihon-u.ac.jp

EMTS 2013 Japan Secretariat:

c/o DUPLER CORP.

3F Sun-Arch Bldg., 3-1 Nemoto, Matsudo,

Chiba 271-0077, Japan

Tel: +81-47-361-6830, Fax: +81-47-388-5372

E-mail: secretariat@ursi-emts2013.org

AP-RASC' 13

2013 Asia-Pacific Radio Science Conference

Howard International House, Taipei, Taiwan, September 3-7, 2013

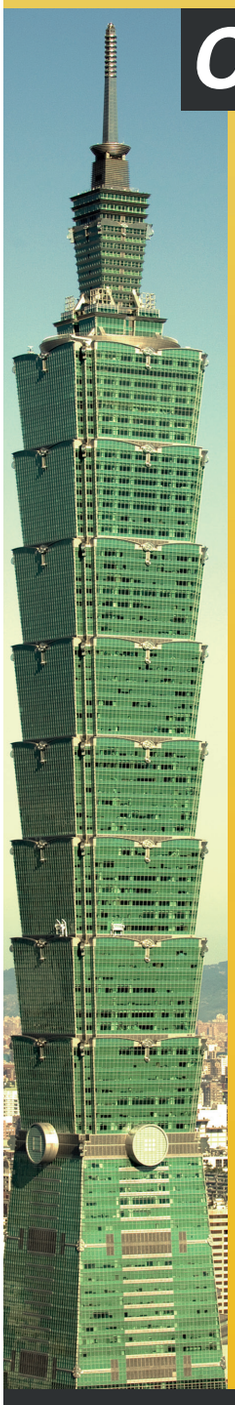

Call for Papers

Website: http://aprasc13.ntu.edu.tw

The "Asia-Pacific Radio Science Conference" (AP-RASC) is the Asia-Pacific regional URSI conference held between the URSI General Assemblies and Scientific Symposia. The objective of the AP-RASC is to review current research trends, present new discoveries, and make plans for future research and special projects in all areas of radio science, especially where international cooperation is desirable, and a particular emphasis is placed on promoting various research activities in the Asia-Pacific area.

Topics

- Electromagnetic Metrology
- Fields and Waves
- Radio Communication and Signal Processing Systems
- Electronics and Photonics
- Electromagnetic Environment and Interference
- Wave Propagation and Remote Sensing
- Ionospheric Radio and Propagation
- Waves in Plasmas
- Radio Astronomy
- Electromagnetics in Biology and Medicine

Young Scientist Programs

As in the URSI General Assemblies and Scientific Symposia, the following two programs are planned for young scientists:

- Student Paper Competition (SPC)
- Young Scientist Award (YSA)

Details on the Programs and the Application Guidelines are posted on the Conference website.

Special Issues

- AP-RASC'13 Special Issue will be published in "Radio Science".
- AP-RASC'13 Special Issue for Student Paper Competition will be published in "URSI Radio Science Bulletin".

Sponsored by

International Union of Radio Science (URSI)
National Taiwan University

In Cooperation with

National Science Council
Academia Sinica
Bureau of Foreign Trade, MOEA
The Institute of Electrical and Electronics Engineers, Inc.(IEEE)

Secretariat

E-mail: ctshih@tl.ntu.edu.tw
Tel: +886-2-23628136 Ext. 49
Fax: +886-2-23632090

Important Dates

Submission Deadline of One-Page Abstracts:
Feb. 28, 2013
Acceptance Notification:
April 30, 2013

Committees

Honorary Conference Chair
Phil Wilkinson, President of URSI, Australia

General Chair
Lou-Chuang Lee, National Central Univ., Taiwan

General Co-Chairs
Shyue-Ching Lu, Chunghwa Telecom. Co., Taiwan
Ruey-Beei Wu, National Taiwan Univ., Taiwan

International Advisory Committee
Co-Chairs:
Kazuya Kobayashi, Chuo Univ., Japan
Lou-Chuang Lee, National Central Univ., Taiwan

International Organizing Committee
Co-Chairs:
Lou-Chuang Lee, National Central Univ., Taiwan
Kazuya Kobayashi, Chuo Univ., Japan

Steering Committee
Chair:
Lou-Chuang Lee, National Central Univ., Taiwan

Organizing Committee
Co-Chairs:
Lou-Chuang Lee, National Central Univ., Taiwan
Shyue-Ching Lu, Chunghwa Telecom. Co., Taiwan
Ruey-Beei Wu, National Taiwan Univ., Taiwan

Technical Program Committee
Co-Chairs:
Hung-Chun Chang, National Taiwan Univ., Taiwan
Yen-Hsyang Chu, National Central Univ., Taiwan

Young Scientist Program Committee
Co-Chairs:
Yen-Hsyang Chu, National Central Univ., Taiwan
Ping-Cheng Yeh, National Taiwan Univ., Taiwan

Secretary
Tzong-Lin Wu, National Taiwan Univ., Taiwan

Electromagnetic Metrology Symposium

Organized by Commission A of the International Union of Radio Science

In coordination with the International Conference on Electromagnetics in Advanced Applications (ICEAA 2013) and the IEEE Topical Conference on Antennas and Propagation in Wireless Communications (IEEE APWC 2013)

September 9 – 13, 2013, Torino, Italy

The first Electromagnetic Metrology Symposium (EMS 2013) is organized by Commission A of the International Union of Radio Science (URSI) in coordination with the ICEAA and IEEE APWC Conferences. The three conferences will be held concurrently at the Torino Incontra Conference Center in Torino, Italy from Monday, September 9 through Friday, September 13, 2013. The three conferences share a common organization, registration fee, submission site, welcoming reception, coffee and lunch breaks, banquet, and social program. Detailed information is found on the conferences website: www.iceaa.org. EMS 2013 will consist of invited and contributed papers, workshops and short courses, and business sessions.

Suggested Topics for EMS
Metrology, measurements and standards in all areas of radio science, including:
Microwave to submillimeter measurements/standards
Quantum metrology and fundamental concepts
Time and frequency
EMC and EM pollution
Noise
Materials
Bioeffects and medical applications
Antennas
EM field metrology
Impulse radar
Planar structures and microstrip circuits
Interconnects and packaging

Information for Authors
Authors must submit a full-page abstract electronically by March 1, 2013. Authors of accepted contributions must register electronically by June 7, 2013. Instructions are found on the website. Each registered author may present no more than two papers. All papers must be presented by one of the authors. Authors who want their paper to be published on IEEE Xplore should follow the instructions on the website. Selected authors of EMS will be invited to submit a full-length paper for possible publication in the URSI Radio Science Bulletin.

Deadlines	Abstract submission	March 1, 2013
	Notification of acceptance	April 12, 2013
	Presenter registration	June 7, 2013

EMS Contacts Prof. William A. Davis, EMS Chair wadavis@vt.edu
Prof. Yasuhiro Koyama, EMS Vice-Chair koyama@nict.go.jp

Inquiries Prof. Roberto D. Graglia, Chair of Organizing Committee roberto.graglia@polito.it
Prof. Piergiorgio L. E. Uslenghi, Chair of Scientific Committee uslenghi@uic.edu

Information for authors

Content

The *Radio Science Bulletin* is published four times per year by the Radio Science Press on behalf of URSI, the International Union of Radio Science. The content of the *Bulletin* falls into three categories: peer-reviewed scientific papers, correspondence items (short technical notes, letters to the editor, reports on meetings, and reviews), and general and administrative information issued by the URSI Secretariat. Scientific papers may be invited (such as papers in the *Reviews of Radio Science* series, from the Commissions of URSI) or contributed. Papers may include original contributions, but should preferably also be of a sufficiently tutorial or review nature to be of interest to a wide range of radio scientists. The *Radio Science Bulletin* is indexed and abstracted by INSPEC.

Scientific papers are subjected to peer review. The content should be original and should not duplicate information or material that has been previously published (if use is made of previously published material, this must be identified to the Editor at the time of submission). Submission of a manuscript constitutes an implicit statement by the author(s) that it has not been submitted, accepted for publication, published, or copyrighted elsewhere, unless stated differently by the author(s) at time of submission. Accepted material will not be returned unless requested by the author(s) at time of submission.

Submissions

Material submitted for publication in the scientific section of the *Bulletin* should be addressed to the Editor, whereas administrative material is handled directly with the Secretariat. Submission in electronic format according to the instructions below is preferred. There are typically no page charges for contributions following the guidelines. No free reprints are provided.

Style and Format

There are no set limits on the length of papers, but they typically range from three to 15 published pages including figures. The official languages of URSI are French and English: contributions in either language are acceptable. No specific style for the manuscript is required as the final layout of the material is done by the URSI Secretariat. Manuscripts should generally be prepared in one column for printing on one side of the paper, with as little use of automatic formatting features of word processors as possible. A complete style guide for the *Reviews of Radio Science* can be downloaded from http://www.ips.gov.au/IPSHosted/NCRS/reviews/. The style instructions in this can be followed for all other *Bulletin* contributions, as well. The name, affiliation, address, telephone and fax numbers, and e-mail address for all authors must be included with

All papers accepted for publication are subject to editing to provide uniformity of style and clarity of language. The publication schedule does not usually permit providing galleys to the author.

Figure captions should be on a separate page in proper style; see the above guide or any issue for examples. All lettering on figures must be of sufficient size to be at least 9 pt in size after reduction to column width. Each illustration should be identified on the back or at the bottom of the sheet with the figure number and name of author(s). If possible, the figures should also be provided in electronic format. TIF is preferred, although other formats are possible as well: please contact the Editor. Electronic versions of figures *must* be of sufficient resolution to permit good quality in print. As a rough guideline, when sized to column width, line art should have a minimum resolution of 300 dpi; color photographs should have a minimum resolution of 150 dpi with a color depth of 24 bits. 72 dpi images intended for the Web are generally *not* acceptable. Contact the Editor for further information.

Electronic Submission

A version of Microsoft *Word* is the preferred format for submissions. Submissions in versions of T_EX can be accepted in some circumstances: please contact the Editor before submitting. *A paper copy of all electronic submissions must be mailed to the Editor, including originals of all figures.* Please do *not* include figures in the same file as the text of a contribution. Electronic files can be send to the Editor in three ways: (1) By sending a floppy diskette or CD-R; (2) By attachment to an e-mail message to the Editor (the maximum size for attachments *after* MIME encoding is about 7 MB); (3) By e-mailing the Editor instructions for downloading the material from an ftp site.

Review Process

The review process usually requires about three months. Authors may be asked to modify the manuscript if it is not accepted in its original form. The elapsed time between receipt of a manuscript and publication is usually less than twelve months.

Copyright

Submission of a contribution to the *Radio Science Bulletin* will be interpreted as assignment and release of copyright and any and all other rights to the Radio Science Press, acting as agent and trustee for URSI. Submission for publication implicitly indicates the author(s) agreement with such assignment, and certification that publication will not violate any other copyrights or other rights associated with the submitted material.

APPLICATION FOR AN URSI RADIOSCIENTIST

I have not attended the last URSI General Assembly, and I wish to remain/become an URSI Radioscientist in the 2012-2014 triennium. Subscription to *The Radio Science Bulletin* is included in the fee.

(please type or print in BLOCK LETTERS)

Name : Prof./Dr./Mr./Mrs./Ms. _____
Family Name First Name Middle Initials

Present job title: _____

Years of professional experience: _____

Professional affiliation: _____

I request that all information be sent to my ☐ home ☐ business address, i.e.:

Company name: _____

Department: _____

Street address: _____

City and postal/zip code: _____

Province/State: _____ Country: _____

Phone: _____ ext._____ Fax: _____

E-mail: _____

Areas of interest (Please tick)

☐ A Electromagnetic Metrology
☐ B Fields and Waves
☐ C Radio-Communication Systems & Signal Processing
☐ D Electronics and Photonics
☐ E Electromagnetic Environment & Interference
☐ F Wave Propagation & Remote Sensing
☐ G Ionospheric Radio and Propagation
☐ H Waves in Plasmas
☐ J Radio Astronomy
☐ K Electromagnetics in Biology & Medicine

I would like to order :

☐ An electronic version of the RSB downloadable from the URSI web site
(The URSI Board of Officers will consider waiving the fee if a case is made to them in writing.) 40 Euro

Method of payment : VISA / MASTERCARD (we do not accept cheques)

Credit card No ☐☐☐☐ ☐☐☐☐ ☐☐☐☐ ☐☐☐☐ Exp. date _____

CVC Code: _____ Date : _____ Signed _____

Please return this signed form to :

The URSI Secretariat
c/o Ghent University / INTEC
Sint-Pietersnieuwstraat 41
B-9000 GHENT, BELGIUM
fax (32) 9-264.42.88